Table 2 Genotype and allele frequencies of CAPN10 polymorphisms in Japanese. The number of subjects of each genotype are indicated. All genotypic distributions are in Hardy-Weinberg equilibrium. *NA* not available, *Ctrl* control, *T2D* type 2 diabetes

Marker	Subjects	Genotype	This study 1	This study 2	This study 3	Horikawa et al. (2003)	Shima et al. (2003)	Daimon et al. (2002)	*P* for heterogeneity
SNP-43	Ctrl	G/G	188	251	165	154	252	76	
		G/A	20	29	24	18	24	5	
		A/A	0	1	0	0	0	0	0.75
		Allele frequency	G: 0.95	G: 0.94	G: 0.94	G: 0.95	G: 0.96	G: 0.97	
			A: 0.05	A: 0.06	A: 0.06	A: 0.05	A: 0.04	A: 0.03	0.62
	T2D	G/G	184	NA	389	158	8	76	
		G/A	21	NA	57	19	2	5	
		A/A	0	NA	1	0	0	0	0.75
		Allele frequency	G: 0.95	NA	G: 0.93	G: 0.95	G: 0.90	G: 0.97	
			A: 0.05		A: 0.07	A: 0.05	A: 0.10	A: 0.03	0.37
Indel-19[a]	Ctrl	2R/2R	27	42	35	23	42	NA	
		2R/3R	99	126	78	78	126	NA	
		3R/3R	82	113	73	71	108	NA	0.90
		Allele frequency	2R: 0.37	2R: 0.37	2R: 0.40	2R: 0.36	2R: 0.38	NA	
			3R: 0.63	3R: 0.63	3R: 0.60	3R: 0.64	3R: 0.62		0.86
	T2D	2R/2R	32	NA	63	28	1	NA	
		2R/3R	104	NA	209	82	3	NA	
		3R/3R	69	NA	176	67	6	NA	0.62
		Allele frequency	2R: 0.41	NA	2R: 0.37	2R: 0.39	2R: 0.25	NA	
			3R: 0.59		3R: 0.63	3R: 0.61	3R: 0.75		0.34
SNP-63	Ctrl	C/C	111	151	99	90	151	NA	
		C/T	81	106	65	70	103	NA	
		T/T	16	24	18	12	22	NA	0.99
		Allele frequency	C: 0.73	C: 0.73	C: 0.72	C: 0.73	C: 0.73	NA	
			T: 0.27	T: 0.27	T: 0.28	T: 0.27	T: 0.27		0.99
	T2D	C/C	90	NA	255	93	6	NA	
		C/T	92	NA	165	74	3	NA	
		T/T	23	NA	30	10	1	NA	0.09
		Allele frequency	C: 0.66	NA	C: 0.75	C: 0.73	C: 0.75	NA	
			T: 0.34		T: 0.25	T: 0.27	T: 0.25		0.03

[a] Indel-19 is a diallelic insertion/deletion polymorphism with alleles of two repeats (2R) or three repeats (3R) of a 32-bp sequence

Table 3 Clinical and metabolic characteristics of normal glucose tolerant subjects (study 2) by SNP-63 genotype. Data are mean ± SD. Subjects underwent a standard 75-g oral glucose tolerance test with glucose and insulin determined at 0′, 30′, 60′, and 120′. The number of individuals in each group for determination of insulinogenic index and HOMA are noted in parentheses. *BMI* body mass index, *AUC* area under the curve

Trait	Genotype			*P*[a]
	C/C	C/T	T/T	
n	150	105	25	
Gender (M/F)	72/78	59/46	14/11	0.40
Age (years)	45.0 ± 14.9	43.8 ± 16.7	44.4 ± 18.7	0.72
BMI (kg/m2)	22.3 ± 2.5	22.2 ± 3.6	22.6 ± 3.0	0.70
HbA1c (%)	4.9 ± 0.4	4.9 ± 0.4	5.0 ± 0.4	0.79
Plasma glucose (mg/dl)				
0 min	93.1 ± 9.6	92.2 ± 9.1	94.1 ± 8.8	0.51
120 min	104.1 ± 18.5	106.1 ± 18.8	108.2 ± 14.5	0.30
AUC 0-120′	14,510.6 ± 2706.2	15,233.4 ± 2937.1	15,043.2 ± 3056.1	0.03
Plasma insulin (μU/ml)				
0 min	6.4 ± 2.2	6.4 ± 2.6	6.5 ± 4.4	0.81
120 min	30.6 ± 16.9	32.0 ± 16.8	30.1 ± 20.2	0.74
AUC 0-120′	3,972.4 ± 2030.8	4,267.4 ± 1816.9	4,049.2 ± 1969.1	0.44
Insulinogenic index	0.89 ± 0.89 (147)	0.96 ± 3.62 (101)	1.14 ± 1.85 (24)	0.08
HOMA	1.43 ± 0.53 (146)	1.41 ± 0.54 (101)	1.30 ± 0.63 (23)	0.35

[a] *P* value by ANCOVA with institution, gender, and genotype as independent factors and age and BMI as covariates

affect the response of the beta cell to aging or its ability to compensate in response to an increasing demand for insulin (Johnson et al. 2004).

The observation that individuals homozygous for the 121 haplotype may be at increased risk of type 2 diabetes in some European populations (Orho-

Table 4 SNP-43, Indel-19, and SNP-63 and type 2 diabetes in Japanese—a pooled analysis. The number of subjects of each genotype are indicated. All genotypic distributions are in Hardy-Weinberg equilibrium. The cases were divided into two groups based on the median age-at-diagnosis in the pooled sample—50 years. Note that age-at-diagnosis was not available for all subjects

Marker	Genotype	Overall			Age-at-diagnosis < 50 years		Age-at-diagnosis ≥50 years	
		Ctrl	T2D	*P*	T2D	*P*	T2D	*P*
SNP-43	G/G	833	811		255		276	
	G/A	91	104		28	0.98	32	0.78
	A/A	0	1	0.35	0		0	
	Allele frequency	G: 0.95	G: 0.94		G: 0.95		G: 0.95	
		A: 0.05	A: 0.06	0.25	A: 0.05	0.98	A: 0.05	0.79
Indel-19[a]	2R/2R	127	124		36		58	
	2R/3R	381	396		143		151	0.11
	3R/3R	334	316	0.67	107	0.33	105	
	Allele frequency	2R: 0.38	2R: 0.39		2R: 0.38		2R: 0.43	
		3R: 0.62	3R: 0.61	0.69	3R: 0.62	0.91	3R: 0.57	0.04
SNP-63	C/C	451	443		149		151	
	C/T	319	333		125		129	
	T/T	68	62	0.72	14	0.09	28	0.35
	Allele frequency	C: 0.73	C: 0.73		C: 0.73		C: 0.71	
		T: 0.27	T: 0.27	0.94	T: 0.27	0.79	T: 0.29	0.17

[a] Indel-19: 2R, 2 repeats of 32-bp sequence; 3R, 3 repeats

Table 5 CAPN10 haplotype frequency and risk of type 2 diabetes in Japanese—a pooled analysis. The haplotypes are those defined by SNP-43, Indel-19, and SNP-63, and the specific alleles are: SNP-43, allele 1, G and allele 2, A; Indel-19, allele 1, 2 repeats of 32-bp sequence, and allele 2, 3 repeats; and SNP-63, allele 1, C, and allele 2, T. The cases were divided into two groups based on the median age-at-diagnosis in the pooled sample—50 years. Note that age-at-diagnosis was not available for all subjects. *Ctrl* control, *T2D* type 2 diabetes

Haplotype	Overall				Age-at-diagnosis < 50 years			Age-at-diagnosis ≥50 years		
	Ctrl ($n=825$)	T2D ($n=827$)	OR (95% CI)[a]	*P*	T2D ($n=277$)	OR (95% CI)[a]	*P*	T2D ($n=305$)	OR (95% CI)[a]	*P*
111	0.106	0.113	1.07 (0.86–1.34)	0.52	0.117	1.12 (0.83–1.52)	0.46	0.136	1.33 (1.00–1.75)	0.05
121	0.572	0.553	0.93 (0.81–1.07)	0.29	0.567	0.98 (0.81–1.19)	0.85	0.515	0.80 (0.66–0.96)	0.02
112	0.270	0.274	1.02 (0.88–1.19)	0.79	0.265	0.98 (0.78–1.21)	0.82	0.297	1.14 (0.93–1.40)	0.21
221	0.052	0.059	1.15 (0.85–1.54)	0.37	0.051	0.97 (0.62–1.50)	0.88	0.052	1.01 (0.66–1.53)	0.97

[a] The OR and 95% CI of each haplotype relative to other haplotypes as a group are shown

Table 6 CAPN10 haplogenotype and risk of type 2 diabetes in Japanese—a pooled analysis. The haplotypes are those defined by SNP-43, Indel-19, and SNP-63, and the specific alleles are indicated in the legend to Table 5. The number of individuals with each haplogenotype is indicated

Haplogenotype	Overall				Age-at-diagnosis < 50 years			Age-at-diagnosis ≥ 50 years		
	Ctrl	T2D	OR (95% CI)[a]	*P*	T2D	OR (95% CI)[a]	*P*	T2D	OR (95% CI)[a]	*P*
111/111	15	18	1.20 (0.60–2.40)	0.60	5	0.99 (0.36–2.76)	0.99	10	1.83 (0.82–4.07)	0.14
111/121	97	93	0.95 (0.70–1.29)	0.74	31	0.95 (0.62–1.45)	0.80	37	1.04 (0.69–1.55)	0.86
111/112	44	44	1.00 (0.65–1.53)	0.99	18	1.23 (0.70–2.17)	0.47	20	1.25 (0.72–2.15)	0.43
111/221	4	14	3.53 (1.24–10.1)	0.02	6	4.54 (1.42–14.5)	0.01	6	4.12 (1.27–13.3)	0.02
112/112	66	62	0.93 (0.65–1.34)	0.70	13	0.57 (0.31–1.04)	0.06	27	1.12 (0.70–1.78)	0.64
112/121	247	254	1.04 (0.84–1.28)	0.73	90	1.13 (0.84–1.51)	0.43	97	1.09 (0.82–1.45)	0.55
112/221	23	32	1.40 (0.82–2.41)	0.22	13	1.72 (0.86–3.41)	0.12	10	1.18 (0.56–2.51)	0.66
121/121	270	259	0.94 (0.76–1.15)	0.54	92	1.02 (0.77–1.37)	0.88	82	0.76 (0.56–1.01)	0.06
121/221	59	50	0.84 (0.57–1.23)	0.37	9	0.44 (0.22–0.87)	0.02	16	0.72 (0.41–1.27)	0.25
221/221	0	1	–	–	0			0		

[a] The OR and 95% CI of each haplogenotype relative to the other haplotype combinations as a group are shown

Melander et al. 2002; Malecki et al. 2002) but at decreased risk in older Japanese raises the possibility that additional genetic variation may distinguish high- and low-risk subtypes of the 121 haplotype. Transpopulation mapping may be a useful strategy for identifying this variation.

Acknowledgements The authors thank Ms. A. Nogami, Ms. M. Y. Sagisaka, and Mr. M. Ikeda for their skillful technical assistance. This study was supported by Grants-in-Aid for Scientific Research C (10671084, 10470234) and for Scientific Research on Priority Areas Medical Genome Science from the Japan Ministry of Science, Education, Sports, Culture and Technology (12204102, 13204082, 14013059, 15012250), Novo Nordisk Foundation, the Naito Foundation (to N.I.) and Grants-in-Aid for Scientific Research B (13470223, 13557091) (to Y.H.), and U.S. Public Health Service (Grants DK-20595, −47486 and −55889). G.I.B. is an Investigator of the Howard Hughes Medical Institute.

References

Abecasis GR, Cookson WO (2000) GOLD–graphical overview of linkage disequilibrium. Bioinformatics 16:182–183

Baier LJ, Permana PA, Yang X, Pratley RE, Hanson RL, Shen GQ, Mott D, Knowler WC, Cox NJ, Horikawa Y, Oda N, Bell GI, Bogardus C (2000) A 1-10 gene polymorphism is associated with reduced muscle mRNA levels and insulin resistance. J Clin Invest 106:R69-R73

Daimon M, Oizumi T, Saitoh T, Kameda W, Yamaguchi H, Ohnuma H, Igarashi M, Manaka H, Kato T (2002) Calpain-10 gene polymorphisms are related, not to type 2 diabetes, but to increased serum cholesterol in Japanese. Diabetes Res Clin Pract 56:147–152

Horikawa Y, Oda N, Cox NJ, Li X, Orho-Melander M, Hara M, Hinokio Y, Lindner TH, Mashima H, Schwarz PE, del Bosque-Plata L, Oda Y, Yoshiuchi I, Colilla S, Polonsky KS, Wei S, Concannon P, Iwasaki N, Schulze J, Baier LJ, Bogardus C, Groop L, Boerwinkle E, Hanis CL, Bell GI (2000) Genetic variation in the gene encoding calpain-10 is associated with type 2 diabetes mellitus. Nat Genet 26:163–175

Horikawa Y, Oda N, Yu L, Imamura S, Fujiwara K, Makino M, Seino Y, Itoh M, Takeda J (2003) Genetic variations in calpain-10 gene are not a major factor in the occurrence of type 2 diabetes in Japanese. J Clin Endocrinol Metab 88:244–247

Iwasaki N, Cox NJ, Wang YQ, Schwarz PE, Bell GI, Honda M, Imura M, Ogata M, Saito M, Kamatani N, Iwamoto Y (2003) Mapping genes influencing type 2 diabetes risk and BMI in Japanese subjects. Diabetes 52:209–213

Johnson JD, Han Z, Otani K, Ye H, Zhang H, Wu H, Horikawa Y, Misler S, Bell GI, Polonsky KS (2004) RyR2 and calpain-10 delineate a novel apoptosis pathway in pancreatic islets. J Biol Chem 279:24794–24802

Malecki MT, Moczulski DK, Klupa T, Wanic K, Cyganek K, Frey J, Sieradzki J (2002) Homozygous combination of calpain 10 gene haplotypes is associated with type 2 diabetes mellitus in a Polish population. Eur J Endocrinol 146:695–699

Mori H, Ikegami H, Kawaguchi Y, Seino S, Yokoi N, Takeda J, Inoue I, Seino Y, Yasuda K, Hanafusa T, Yamagata K, Awata T, Kadowaki T, Hara K, Yamada N, Gotoda T, Iwasaki N, Iwamoto Y, Sanke T, Nanjo K, Oka Y, Matsutani A, Maeda E, Kasuga M (2001) The Pro12 → Ala substitution in PPAR-γ is associated with resistance to development of diabetes in the general population: possible involvement in impairment of insulin secretion in individuals with type 2 diabetes. Diabetes 50:891–894

Mori Y, Otabe S, Dina C, Yasuda K, Populaire C, Lecoeur C, Vatin V, Durand E, Hara K, Okada T, Tobe K, Boutin P, Kadowaki T, Froguel P (2002) Genome-wide search for type 2 diabetes in Japanese affected sib-pairs confirms susceptibility genes on 3q, 15q, and 20q and identifies two new candidate Loci on 7p and 11p. Diabetes 51:1247–1255

Orho-Melander M, Klannemark M, Svensson MK, Ridderstrale M, Lindgren CM, Groop L (2002) Variants in the calpain-10 gene predispose to insulin resistance and elevated free fatty acid levels. Diabetes 51:2658–2664

Seino S on behalf of the Study Group of Comprehensive Analysis of Genetic Factors in Diabetes Mellitus (2001) S20G mutation of the amylin gene is associated with Type II diabetes in Japanese. Diabetologia 44:906–909

Shima Y, Nakanishi K, Odawara M, Kobayashi T, Ohta H (2003) Association of the SNP-19 genotype 22 in the calpain-10 gene with elevated body mass index and hemoglobin A1c levels in Japanese. Clin Chim Acta 336:89–96

Song Y, Niu T, Manson JE, Kwiatkowski DJ, Liu S (2004) Are variants in the CAPN10 gene related to risk of type 2 diabetes? A quantitative assessment of population and family-based association studies. Am J Hum Genet 74:208–222

Weedon MN, Schwarz PE, Horikawa Y, Iwasaki N, Illig T, Holle R, Rathmann W, Selisko T, Schulze J, Owen KR, Evans J, Del Bosque-Plata L, Hitman G, Walker M, Levy JC, Sampson M, Bell GI, McCarthy MI, Hattersley AT, Frayling TM (2003) Meta-analysis and a large association study confirm a role for calpain-10 variation in type 2 diabetes susceptibility. Am J Hum Genet 73:1208–1212

0021-972X/05/$15.00/0
Printed in U.S.A.

The Journal of Clinical Endocrinology & Metabolism 90(9):5401–5406

doi: 10.1210/jc.2005-0202

Severe Congenital Hyperinsulinism Caused by a Mutation in the Kir6.2 Subunit of the Adenosine Triphosphate-Sensitive Potassium Channel Impairing Trafficking and Function

Eric Marthinet, Alain Bloc, Yoshimoto Oka, Yukio Tanizawa, Bernhard Wehrle-Haller, Victor Bancila, Jean-Michel Dubuis, Jacques Philippe, and Valerie M. Schwitzgebel

Pediatric Endocrinology and Diabetology (E.M., J.-M.D., V.M.S.) and Diabetes Unit (E.M., J.P.), University Hospital of Geneva, and Departments of Neuroscience (A.B., V.B.) and Cellular Physiology and Metabolism (B.W.-H.), University of Geneva, CH-1211 Geneva, Switzerland; Biochemical Institute (A.B.), University of Lausanne, CH-1015 Lausanne, Switzerland; Department of Internal Medicine (Y.O.), Tohoku University Graduate School of Medicine Seiryo-machi, Sendai 980-8575, Japan; and Division of Molecular Analysis of Human Disorders (Y.T.), Yamaguchi University Graduate School of Medicine, Ube 755-8505, Japan

Context: The ATP-sensitive potassium (K_{ATP}) channel, assembled from the inwardly rectifying potassium channel Kir6.2 and the sulfonylurea receptor 1, regulates insulin secretion in β-cells. A loss of function of K_{ATP} channels causes depolarization of β-cells and congenital hyperinsulinism (CHI), a disease presenting with severe hypoglycemia in the newborn period.

Objective: Our objective was identification of a novel mutation in Kir6.2 in a patient with CHI and molecular and cell-biological analysis of the impact of this mutation.

Design and Setting: We combined immunohistochemistry, advanced life fluorescence imaging, and electrophysiology in HEK293T cells transiently transfected with mutant Kir6.2.

Patient and Intervention: The patient presented with macrosomia at birth and severe hyperinsulinemic hypoglycemia. Despite medical treatment, the newborn continued to suffer from severe hypoglycemic episodes, and at 4 months of age subtotal pancreatectomy was performed.

Main Outcome Measure: We assessed patch-clamp recordings and confocal microscopy in HEK293T cells.

Results: We have identified a homozygous missense mutation, H259R, in the Kir6.2 subunit of a patient with severe CHI. Coexpression of $Kir6.2_{H259R}$ with sulfonylurea receptor 1 in HEK293T cells completely abolished K_{ATP} currents in electrophysiological recordings. Double immunofluorescence staining revealed that mutant Kir6.2 was partly retained in the endoplasmic reticulum (ER) causing decreased surface expression as observed with total internal reflection fluorescence. Mutation of an ER-retention signal partially rescued the trafficking defect without restoring whole-cell currents.

Conclusion: The H259R mutation of the Kir6.2 subunit results in a channel that is partially retained in the ER and nonfunctional upon arrival at the plasma membrane. (***J Clin Endocrinol Metab* 90: 5401–5406, 2005**)

K_{ATP} CHANNELS COUPLE the metabolism of a cell to its electrical activity and are widely expressed. In the heart, these channels are involved in ischemic preconditioning (1), whereas in the brain, they have neuroprotective roles during ischemia (2). In the pancreas, K_{ATP} channels are localized at the plasma membrane of β-cells and to the insulin secretory granule (3), where they sense ATP, which is tightly regulated by glucose levels. Thus, an increase in glucose concentration leads to a higher ATP to ADP ratio and to K_{ATP} closure, β-cell depolarization, and insulin secretion. The functional K_{ATP} channel is an octameric complex formed by four sulfonylurea receptor 1 (SUR1) and four inwardly rectifying Kir6.2 subunits (4). Chronically impaired channel function causes depolarization of the β-cell with sustained insulin secretion, a condition known as congenital hyperinsulinism (CHI), previously termed as persistent hyperinsulinemic hypoglycemia of infancy. Histologically, two different forms of CHI exist, a diffuse form, where all the islets of the pancreas are altered, and a focal form with a small region of hyperplastic β-cells surrounded by normal pancreatic islets (5). Overall, 40–65% of patients with CHI present a focal form (6–8). A majority of studies have identified mutations in the SUR1 subunit associated with CHI (9, 10). To date, more than 10 Kir6.2 mutations have been identified with CHI (11–16). One Kir6.2 mutation (Y12X) caused the synthesis of a truncated nonfunctional protein (12), whereas another mutation (W91R) showed defective channel assembly with a rapid degradation in the endoplasmic reticulum (ER) (17).

Here we identified a new homozygous mutation in the Kir6.2 subunit in a patient with severe CHI. Combining immunohistochemistry, advanced life fluorescence imaging, and electrophysiology, we demonstrate that the H259R mutation leads to a nonfunctional K_{ATP} channel and impaired trafficking to the cell membrane.

First Published Online July 5, 2005

Abbreviations: CHI, Congenital hyperinsulinism; EGFP, enhanced green fluorescent protein; ER, endoplasmic reticulum; HBA_{1c}, glycosylated hemoglobin; K_{ATP}, ATP sensitive K^+ channel; SUR1, sulfonylurea receptor 1; TIRF, total internal reflection fluorescence; WT, wild type.

Patient and Methods

Genetic analysis

Genomic DNA was extracted from peripheral blood using the genomic PrepBlood DNA isolation kit (Amersham Pharmacia Biotech, Piscataway, NJ) after informed consent had been obtained. Individual exons of the *ABCC8* gene coding for SUR1 (39 exons) and the *KCNJ11* gene coding for Kir6.2 (1 exon) (GenBank accession numbers L78207 for *ABCC8* and NM_000525 for *KCNJ11*) were amplified by PCR and screened for mutations by direct nucleotide sequencing (18).

Molecular biology

The plasmid pECE-*hKir6.2* [wild type (WT)] (a generous gift from Dr. J. Bryan, Baylor College of Medicine, Houston, TX) was used to generate the pECE-*hKir6.2* (H259R) using the *in vitro* QuikChange site-directed mutagenesis kit (Stratagene, Amsterdam, The Netherlands) according to the manufacturer's protocol. The following primers were used: forward, 5′-CCGCTGATCATCTACCGTGTCATTGATGCCAACAGC-3′, and reverse, 5′-GCTGTTGGCATCAATGACACGGTAGATGATCAGCGG-3′. The mutation was confirmed by DNA sequencing. WT and mutant *KCNJ11* cDNA were subcloned into the pCDNA3 vector (Invitrogen, Basel, Switzerland). The pCDNA3-*hKir6.2*(WT) and the pCDNA3-*hKir6.2*(H259R) were used to generate pcDNA3-*hKir6.2*$_{AAA}$(WT) and the pCDNA3-*hKir6.2*$_{AAA}$(H259R) with the *in vitro* QuikChange site-directed mutagenesis kit by using the following primers: forward, 5′-CCGCGGGCCCCTGGCCGCGGCCAGCGTGCCCATGG-3′, and reverse, 5′-CCATGGGCACGCTGGCCGCGGCCAGGGGCCCGCGG-3′. All the mutations were confirmed by DNA sequencing. Human ABCC8 cDNA (pECE-*hSUR1* (a generous gift from Dr. J. Bryan) was subcloned into the pCDNA3 vector.

Cell culture and transfections

The human embryonic kidney (HEK293T) cell line was grown and maintained in RPMI 1640 (Seromed, Basel, Switzerland) supplemented with 5% fetal calf serum, 5% newborn calf serum (Life Technologies, Basel, Switzerland), 100 U/ml penicillin (Seromed), 100 μg/ml streptomycin (Seromed), and 2 mM glutamine (Life Technologies). HEK293T cells were transiently cotransfected using the calcium phosphate precipitation technique with human *ABCC8* and *KCNJ11* cDNA (WT, WT_{AAA}, H259R, and $H259R_{AAA}$) in a 4:1 ratio (1 μg of *ABCC8* and 0.25 μg of *KCNJ11*) (19). After 48 h, cells were used for the patch clamp technique, for immunohistochemistry or total internal reflection fluorescence (TIRF) microscopy experiments. We transfected HEK293T cells with two enhanced green fluorescent protein (EGFP) fusion constructs [Kitl-EGFP (Mb-EGFP) and KLS-EGFP (ER-EGFP)] to label either the cell membrane or the ER, using the same conditions as described previously, to validate our TIRF experiments (20).

Electrophysiological measurements

As described previously (21), all experiments were performed at room temperature (20–22 C). The pipette solution consisted of 10 mM NaCl, 140 mM KCl, 1 mM $MgCl_2$, 10 mM HEPES, 1 mM EGTA, 1 mM MgATP (pH 7.2 with KOH), and the extracellular solution used was 145 mM NaCl, 3 mM KCl, 2 mM $CaCl_2$, 2 mM $MgCl_2$, 10 mM HEPES, 10 mM D-glucose (pH 7.2 with NaOH). The equilibrium potential for K^+ ions (E_K) was −82 mV. Membrane slope conductance values (G_m) were calculated from dI/dV, using ramp voltage-clamp protocol (between −120 and −40 mV, a voltage range symmetrical to E_K). dI was determined from tolbutamide-sensitive currents.

Immunohistochemistry

HEK293T cells were stained with the following antibodies: goat anti-Kir6.2 (sc11228; Santa Cruz Biotechnology, Heidelberg, Germany), guinea pig anti-Kir6.2 (generous gift from Dr. B. Schwappach), and goat anticalreticulin (generous gift from Dr. M. Michalak) to mark the ER and mouse antigiantin (generous gift from Drs. H. Hauri and M. Spiess) to stain the Golgi apparatus. The following secondary antibodies were used: antigoat fluorescein isothiocyanate, antimouse Alexa568, and antigoat alexa 568 (Molecular Probes, Leiden, The Netherlands). For colocalization experiments of the protein Kir6.2 with the plasmic membrane marker, toxin-GPI-alexa546 (generous gift from Dr. F. van der Goot) was used. Slides were viewed on a Zeiss LSM 510 confocal microscope (Carl Zeiss AG, Göttingen, Germany).

TIRF microscopy

We used an inverted microscope Axiovert 100M (Carl Zeiss) equipped with a high numerical aperture objective (×100 NA 1.45; Carl Zeiss) and a combined epifluorescence/TIRF adapter (TILL Photonics, Gräfelfing, Germany). Fluorophores were excited at 488 nm with a 150-mW argon-ion laser through a monomode optical fiber (488/568/647 nm) and the fluorescence filter set containing a laser clean-up filter (488/10), dichroic mirror (DCLP500), and band pass emission filter (BP525/50). Images were acquired with a 12-bit CCD camera (Orca 9742-95; Hamamatsu, Hamamatsu City, Japan). The laser shutter, the camera and the microscope set up were controlled by the Openlab software (Improvision, Basel, Switzerland).

Quantification and statistical analysis

The percentage of colocalization of the protein Kir6.2 (WT or H259R) with the different markers used in this study was calculated with the Metamorph software version 6.2r4 (Universal Imaging, Puchheim, Germany). Results are expressed as mean ± SD. Where indicated, the statistical significance of the differences between groups was estimated by the Mann-Whitney U test or the t test. Statistical significance is indicated as follows: *, $P < 0.01$; **, $P < 0.001$.

Results

Case synopsis

The infant was born at term after an uneventful pregnancy and presented with macrosomia (body weight, 4460 g; body length, 54 cm; both values are above the 90th percentile). Thirty minutes after birth, severe hypoglycemic episodes were observed [glucose level of 31 mg/dl (1.7 mmol/liter) with a simultaneous insulin level of 172 mU/liter] leading to the diagnosis of hyperinsulinism. The newborn was treated with iv glucose at a rate of 20 mg/kg·min, and diazoxide was added at a dose of 17 mg/kg·d. Despite treatment, the newborn continued to suffer from severe hypoglycemic episodes, and octreotide (17 μg/kg·d) and nifedipine (0.25 mg/kg·d) were added successively without therapeutic success. Continuous iv glucagon (1 mg/d) was needed to stabilize the blood glucose levels. The patient developed clinical signs of cardiac insufficiency; cardiac ultrasound showed biventricular hypertrophy. At 4 months of age a pancreatic catheterization with measurements of insulin levels (6) suggested a diffuse form of CHI. At 5 months of age, a subtotal pancreatectomy (95%) was performed, and pancreatic histopathology confirmed the diagnosis. After pancreatectomy, the infant became diabetic and was treated with an insulin pump. At the age of 20 months the total daily insulin dose was 0.54 U/kg with a glycosylated hemoglobin (HbA_{1c}) of 6.9%. Blood glucose measurements showed maximal levels of 181 mg/dl (10 mmol/liter). The insulin dose was gradually tapered and eventually stopped at the age of 23 months. Two months after the insulin treatment was completely stopped, the HbA_{1c} was at 6.4%, and daily blood glucose measurements varied between 74.5 mg/dl (4.1 mmol/liter) and 145 mg/dl (8 mmol/liter). The HbA_{1c} values further decreased to 5.4% at the age of 36 months without any treatment, and no hypoglycemic episodes were encountered.

Genetic analysis

Sequencing of the 39 exons of the *ABCC8* gene, encoding the SUR1 protein, revealed no mutation. In contrast, a homozygous missense mutation, 776A→G, was found in the *KCNJ11* gene, encoding the Kir6.2 protein, leading to a change in the amino acid sequence (H259R). The mutation was located close to the C-terminal end at a highly conserved site, found in 52 proteins related to Kir6.2. This makes DNA sequence polymorphism therefore unlikely (Fig. 1). Both parents were found to be heterozygous for the 776A→G mutation.

Functional analysis of the mutant K_{ATP} channel

To study the functional impact of the mutation in the Kir6.2 protein on the K_{ATP} channel, we used the patch clamp technique in the whole-cell configuration. HEK293T cells were transiently cotransfected with mutant *KCNJ11* cDNA and wild-type *ABCC8* cDNA. GFP cDNA was added to identify successfully transfected cells. As shown in Fig. 2, K_{ATP} currents were absent in cells expressing the mutant K_{ATP} channel (Fig. 2B) but present in the WT (Fig. 2A). Earlier studies have reported that functional recovery of K_{ATP} currents in the case of mutation in the SUR1 subunits can be obtained with diazoxide (22). As shown in Fig. 2B (*middle*), diazoxide had no effect on the H259R mutant K_{ATP} channel. In fact, the current was completely absent in all cells with the mutated K_{ATP} channel ($n = 8$; $P < 0.001$) (Fig. 2, B and C).

Retention of mutant K_{ATP} channel in the ER

The absence of current could result from several abnormalities such as decreased protein synthesis, defects in assembly and trafficking, increased degradation (17), or impaired function of the channel itself (23). In our case, the H259R mutation did not appear to interfere with protein synthesis, because Kir6.2 protein could be synthesized *in vitro* (data not shown). It has been shown that K_{ATP} channels are subjected to quality control during ER trafficking, whereby the correct assembly of the subunits masks retention signals (24, 25) and allows membrane insertion. To test for trafficking defects of the mutant Kir6.2, we performed immunohistochemical costaining experiments with markers of the ER and the Golgi apparatus. Costaining with antibodies against the calreticulin protein of the ER revealed a 2-fold increase in colocalization of the mutant channel (42.6 ± 8.8%; n = 11) in comparison with WT (22.3 ± 7.7%; n = 11) (Fig. 3). The same results were obtained with the colocalization of the Kir6.2 protein with the ER-EGFP (data not shown). In contrast, costaining with antisera against the Golgi apparatus showed no difference in comparison with WT (1.3 ± 0.1%, n = 4, *vs.* 1.7 ± 0.3%, n = 5) (Fig. 4). We conclude from these experiments that a significant amount of mutant Kir6.2 is retained in the ER, and as a consequence there is a reduced expression of the mutant K_{ATP} channel at the cell membrane.

We therefore tested whether the additional mutation of the ER retention signal RKR to AAA rescued K_{ATP} channels. As expected, this led to a significant decrease of fluorescence that colocalized with the ER marker calreticulin (13.1 ± 4.9% *vs.* 42.6 ± 8.8%; n = 8–11 cell; $P < 0.01$; data not shown). However, even after elimination of the ER retention signal, no K_{ATP} currents were recorded (Fig. 5, A and B) ($n = 7$; $P < 0.01$). Furthermore diazoxide applied to cells transfected with $H259R_{AAA}$ still did not restore K_{ATP} currents (Fig. 5C). In contrast, in WT_{AAA}-transfected cells, diazoxide enhanced K_{ATP} currents.

Reduced expression of the mutant K_{ATP} channel at the cellular membrane

This conclusion is further supported by confocal images showing a marked reduction in membrane staining of the mutant Kir6.2 K_{ATP} channel compared with WT. Costaining with the plasmic membrane marker, toxin-GPI-alexa546, revealed a reduced colocalization of the mutant channel with the plasma membrane (9.5 ± 1.5%; n = 3) in comparison with WT (14.5 ± 1.3%; n = 3) (Fig. 6). Finally, these results were confirmed by TIRF imaging, which allows selective visualization of fluorescence localized at the cell surface. Again, expressing the mutant KCNJ11 cDNA led to a significantly lower signal of the protein at the cell surface compared with WT (Fig. 7A). To validate our TIRF experiments and to decrease the likelihood that the fluorescence signal obtained may relate to channels close to the membrane, we transfected HEK293T with two GFP fusion constructs, localizing either to the plasma membrane (Mb-EGFP) or to the ER (ER-EGFP) (20) (Fig. 7B). The fluorescence observed in TIRF with the membrane marker Mb-EGFP is comparable with the fluorescence obtained with Kir6.2 WT. The TIRF fluorescence of the ER-EGFP protein is similar to the one seen with the mutant H259R protein. Taken together, these results thus show that the mutant Kir6.2 is partially retained in the ER, but a fraction still reaches the cell membrane.

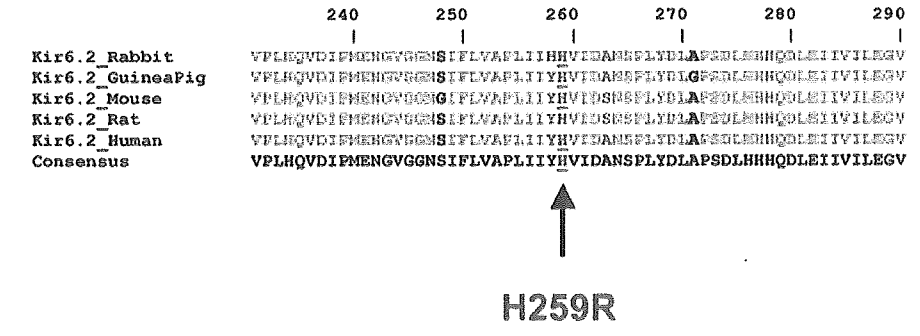

FIG. 1. Identification of a new point mutation H259R in the C terminus of the Kir6.2 protein in the index patient. Protein sequence alignment of the region containing the mutation shows the conservation of the mutated amino acid between species.

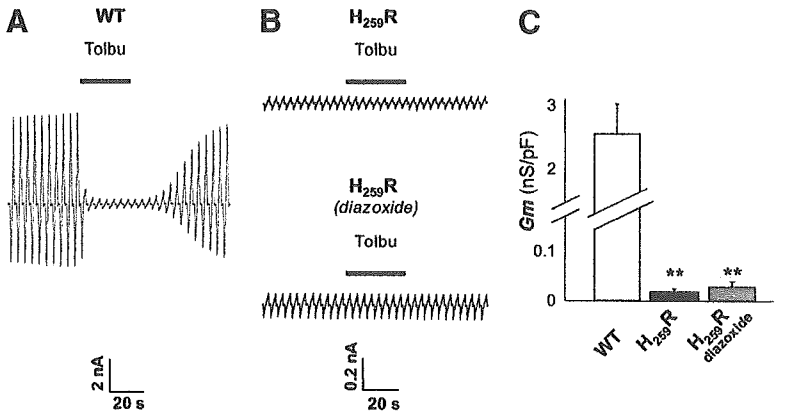

FIG. 2. Functional analysis of mutated K_{ATP} channel. A, Whole-cell currents recorded in response to ramps of voltage from −120 to −40 mV over a 3-sec period from voltage-clamped HEK293T cells (holding potential, −80 mV) coexpressing Kir6.2WT plus SUR1. B, Kir6.2H259R plus SUR1 and Kir6.2H259R plus SUR1 after an incubation with 200 μM diazoxide for 48 h. Cells were continuously perfused with extracellular solution (see *Materials and Methods*) during the course of the recording, and 250 μM tolbutamide (tolbu) was added when indicated to block recombinant K_{ATP} currents and allow quantification of their amplitude. C, Membrane slope conductance values (*Gm* as mean ± SD) calculated for each type of recombinant channel expressed in HEK293T cells: Kir6.2WT plus SUR1 (n = 9 cells); Kir6.2H259R plus SUR1 (n = 8 cells); Kir6.2H259R plus SUR1 submitted to a 48-h treatment with diazoxide (n = 8 cells) ($P < 0.001$).

Discussion

We describe a human mutation located at the C terminus of Kir6.2 that impairs trafficking and abolishes channel function. Immunohistochemical visualization of mutated Kir6.2 revealed a decreased surface pool, whereas fluorescence in the ER was enhanced. In addition, whole-cell currents were abolished, which suggests that the fraction of channels that eventually reaches the surface is not functional. This conclusion is also supported by the nonresponsiveness to diazoxide in the patch clamp experiments.

During biosynthesis, the Kir6.2 protein is exported from the ER only if properly assembled into an octameric K_{ATP} channel (24). In fact, the formation of the Kir6.2 tetramer leads to the masking of an ER-retention signal located in the cytoplasmic tail of the Kir6.2 protein. Mutation analysis indicates that the ER-retention signals contain a -RKR- motif (24). Assembly of functional channels that reach the surface will occur only after a second retention signal located on the SUR subunit is subsequently masked. An alternate assembly model proposes the formation of a SUR-Kir6.2 heterodimer before the octamer formation (17). Our data are compatible with both assembly models. In fact, the H259R mutation may interfere in several ways with this quality control mechanism. First, the H259R mutation may have created a new retention signal, a possibility that, however, is not very likely because the mutation did not create any of the established retention motifs including -RXR- (26). Second, the -RKR- motif could have been indirectly inactivated by the H259R mutation through a change of the tertiary conformation of the Kir6.2 protein. This would cause an inappropriate trafficking of $Kir6.2_{H259R}$ tetramers to the cell surface without the need to coassemble with SUR just as C-terminally truncated Kir6.2 proteins are inserted into the membrane (24, 27). Again, this scenario seems unlikely because such C-terminally truncated tetramers constitute functional channels, whereas the H259R mutation led to a complete absence of currents. Therefore, we favor a model whereby the H259R mutation would change the conformation of the Kir6.2 protein in a way that would prevent the complete masking of the retention signal that normally occurs during assembly (24, 28). This model could explain partial retention in the ER that can be overcome by mutating the RKR sequence. As a consequence, only a fraction of the mutated channels is expressed at the surface. The mutation may cause structural alteration abolishing function, for example by affecting ATP gating, which may provide an explanation why even in the presence of surface fluorescence, no currents were recorded. In line with this interpretation, mutating the ER retention signal RKR in Kir6.2 to AAA did not rescue K_{ATP} currents.

A similar dual defect was reported for the ΔF1388 mutation in the SUR1 subunit; this mutation caused defective trafficking and lack of surface expression (29). Additional experiments led to the conclusion that even if expressed at the surface, the ΔF1388 mutation interfered with K_{ATP} func-

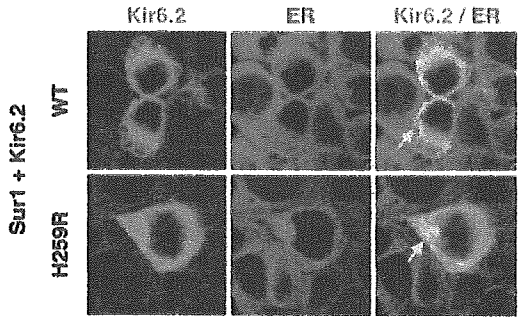

FIG. 3. Coexpression of WT and mutant K_{ATP} channel with markers for the ER. HEK293T cells were cotransfected with SUR1 and Kir6.2WT or SUR1 and Kir6.2H259R. Double immunofluorescence staining showed a 2-fold increase in colocalization of the mutant K_{ATP} channel with the calreticulin protein in the ER (*yellow staining, arrow*) in comparison with WT. Photomicrographs were imaged confocally.

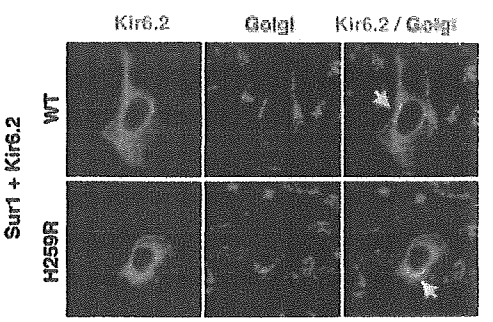

FIG. 4. Coexpression of WT and mutant K_{ATP} channel with markers for the Golgi apparatus. HEK293T cells were cotransfected with SUR1 and Kir6.2WT or SUR1 and Kir6.2H259R. Double immunofluorescence staining of the mutant K_{ATP} channel with the giantin protein of the Golgi apparatus (*yellow staining, arrow*) showed no difference in comparison with WT. Photomicrographs were imaged confocally.

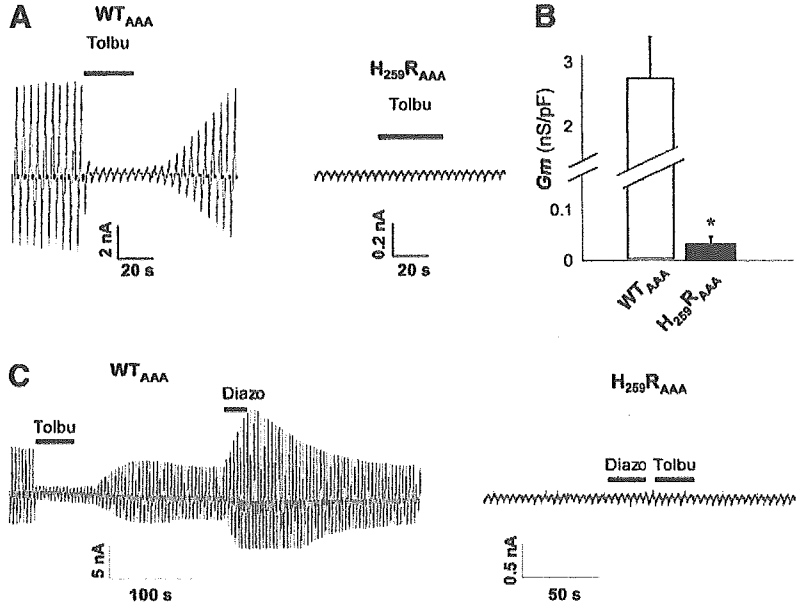

FIG. 5. Functional analysis of mutated K_{ATP} channel devoid of the RKR retention signal. A, Whole-cell currents recorded in response to ramps of voltage from −120 to −40 mV over a 3-sec period from voltage-clamped HEK293T cells (holding potential, −80 mV) coexpressing either Kir6.2WT$_{AAA}$ plus SUR1 or Kir6.2H259R$_{AAA}$ plus SUR1. B, Membrane slope conductance values (*Gm* as mean ± SD) calculated for each type of recombinant channel expressed in HEK293T cells: Kir6.2WT$_{AAA}$ plus SUR1 (n = 8 cells); Kir6.2H259R$_{AAA}$ plus SUR1 (n = 7 cells) ($P < 0.01$). C, *Bars* indicate application of diazoxide (diazo; 100 μM) and tolbutamide (tolbu; 250 μM). Diazoxide applied to cells transfected with H259R$_{AAA}$ did not restore K_{ATP} currents. In contrast, in WT$_{AAA}$-transfected cells, diazoxide enhanced K_{ATP} currents.

tion. The severity and the early onset of hypoglycemia in the case described here may reflect the complete loss of channel function revealed in this study. Moreover, the patient was resistant to diazoxide, an observation mirrored by the absence of an effect of diazoxide in the electrophysiological recordings (22).

The observation that diabetes resolved 18 months after subtotal pancreatectomy is unusual and could potentially be explained by a partial regeneration of the pancreas as previously reported (30, 31). We assume that the number of β-cells has increased during pancreas regeneration and that the amount of secreted insulin is sufficient to avoid overt hyperglycemia. The child is still on a strict diet with three main meals and three snacks, including one at bedtime, which could help to avoid severe hypoglycemic episodes, secondary to inappropriate insulin secretion. It is possible that our index case experiences unrecognized hypoglycemic episodes.

K_{ATP} channels containing the Kir6.2 subunit are present in the pancreatic β-cell, the brain, the cardiomyocyte, and the smooth muscle (32–36); the targeted disruption of Kir6.2 in mice showed exercise-induced arrhythmia and sudden cardiac death (1). We therefore recorded an electrocardiogram over a 24-h period, which included a period of exercise; however, no arrhythmia was noted and the QT interval was normal. Despite severe hypoglycemic episodes during infancy, the child is developing normally at 4 yr of age and has a normal statural growth. Loss of function of Kir6.2 in the

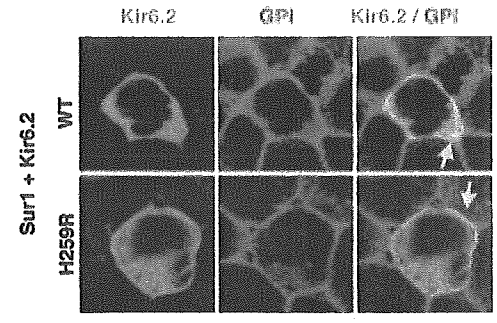

FIG. 6. Reduced surface expression of mutant H259R-K_{ATP} channel. HEK293T cells were cotransfected with SUR1 and Kir6.2WT or SUR1 and Kir6.2H259R. Colocalization of the wild-type or mutant K_{ATP} channel and the membrane marker, toxin-GPI-alexa546, was visualized by confocal imaging. Double immunofluorescence staining revealed decreased membrane expression (*yellow staining, arrow*) for the mutant K_{ATP} channel in comparison with WT.

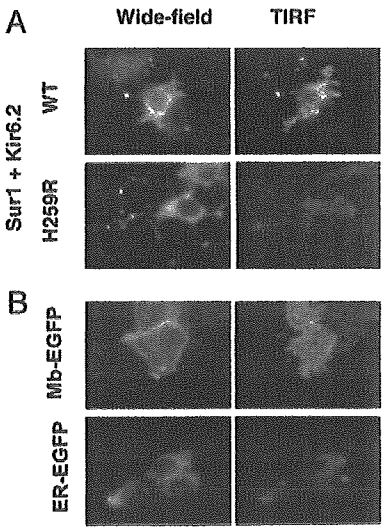

FIG. 7. Wide-field fluorescence and TIRF fluorescence were visualized for the WT K_{ATP} and the mutant K_{ATP} channel. A, The same cell is shown with the wide-field and with TIRF technique (WT in the *upper panel* and H259R in the *lower panel*). The TIRF technique showed expression of the WT K_{ATP} channel at the surface (*white arrows*), whereas the mutant K_{ATP} expression was markedly reduced. B, Wide-field fluorescence and TIRF fluorescence were visualized for the Mb-EGFP and the ER-EGFP. The same cell is shown with the wide-field and with TIRF technique (Mb-EGFP in the *upper panel* and ER-EGFP in the *lower panel*). The TIRF technique showed expression of the Mb-EGFP at the surface, whereas the ER-EGFP expression at the surface was very weak.

human brain seems not to interfere with normal development. It is possible that other inwardly rectifying potassium channels substitute for the neuronal loss of Kir6.2. Kir6.1, however, seems an unlikely candidate because it is mainly expressed in astrocytes (37). However, the child could be at risk for hypoxia-induced seizures, as described in Kir6.2$^{-/-}$ mice (2). The parents, both heterozygous for the H259R mutation, never experienced hypoglycemic episodes, excluding a dominant negative effect of H259R.

In conclusion, we identify histidine 259 as an important residue in the C terminus of human Kir6.2 protein that affects trafficking and is required for channel function.

Acknowledgments

We thank Dr. Gilian Friedli, Dr. Beat Friedli, and Dr. C. Le Coultre for their collaboration.

Received January 31, 2005. Accepted June 24, 2005.

Address all correspondence and requests for reprints to: Valérie M. Schwitzgebel, Pediatric Endocrinology and Diabetology, Children's Hospital, 6, rue Willy Donzé, CH-1211 Geneva, Switzerland. E-mail: valerie.schwitzgebel@hcuge.ch.

This work was supported by the Swiss National Science Foundation (Grant 3200-065162.01).

References

1. **Zingman LV, Hodgson DM, Bast PH, Kane GC, Perez-Terzic C, Gumina RJ, Pucar D, Bienengraeber M, Dzeja PP, Miki T, Seino S, Alekseev AE, Terzic A** 2002 Kir6.2 is required for adaptation to stress. Proc Natl Acad Sci USA 99:13278–13283
2. **Yamada K, Ji JJ, Yuan H, Miki T, Sato S, Horimoto N, Shimizu T, Seino S, Inagaki N** 2001 Protective role of ATP-sensitive potassium channels in hypoxia-induced generalized seizure. Science 292:1543–1546
3. **Geng X, Li L, Watkins S, Robbins PD, Drain P** 2003 The insulin secretory granule is the major site of K(ATP) channels of the endocrine pancreas. Diabetes 52:767–776
4. **Clement 4th JP, Kunjilwar K, Gonzalez G, Schwanstecher M, Panten U, Aguilar-Bryan L, Bryan J** 1997 Association and stoichiometry of K(ATP) channel subunits. Neuron 18:827–838
5. **Sempoux C, Guiot Y, Dahan K, Moulin P, Stevens M, Lambot V, de Lonlay P, Fournet JC, Junien C, Jaubert F, Nihoul-Fekete C, Saudubray JM, Rahier J** 2003 The focal form of persistent hyperinsulinemic hypoglycemia of infancy: morphological and molecular studies show structural and functional differences with insulinoma. Diabetes 52:784–794
6. **de Lonlay-Debeney P, Poggi-Travert F, Fournet JC, Sempoux C, Vici CD, Brunelle F, Touati G, Rahier J, Junien C, Nihoul-Fekete C, Robert JJ, Saudubray JM** 1999 Clinical features of 52 neonates with hyperinsulinism. N Engl J Med 340:1169–1175
7. **Glaser B, Ryan F, Donath M, Landau H, Stanley CA, Baker L, Barton DE, Thornton PS** 1999 Hyperinsulinism caused by paternal-specific inheritance of a recessive mutation in the sulfonylurea-receptor gene. Diabetes 48:1652–1657
8. **Stanley CA** 2002 Advances in diagnosis and treatment of hyperinsulinism in infants and children. J Clin Endocrinol Metab 87:4857–4859
9. **Thomas PM, Cote GJ, Wohllk N, Haddad B, Mathew PM, Rabl W, Aguilar-Bryan L, Gagel RF, Bryan J** 1995 Mutations in the sulfonylurea receptor gene in familial persistent hyperinsulinemic hypoglycemia of infancy [see comments]. Science 268:426–429
10. **Dunne MJ, Cosgrove KE, Shepherd RM, Aynsley-Green A, Lindley KJ** 2004 Hyperinsulinism in infancy: from basic science to clinical disease. Physiol Rev 84:239–275
11. **Thomas P, Ye Y, Lightner E** 1996 Mutation of the pancreatic islet inward rectifier Kir6.2 also leads to familial persistent hyperinsulinemic hypoglycemia of infancy. Hum Mol Genet 5:1809–1812
12. **Nestorowicz A, Inagaki N, Gonoi T, Schoor KP, Wilson BA, Glaser B, Landau H, Stanley CA, Thornton PS, Seino S, Permutt MA** 1997 A nonsense mutation in the inward rectifier potassium channel gene, Kir6.2, is associated with familial hyperinsulinism. Diabetes 46:1743–1748
13. **Aguilar-Bryan L, Bryan J** 1999 Molecular biology of adenosine triphosphate-sensitive potassium channels. Endocr Rev 20:101–135
14. **Huopio H, Jaaskelainen J, Komulainen J, Miettinen R, Karkkainen P, Laakso M, Tapanainen P, Voutilainen R, Otonkoski T** 2002 Acute insulin response tests for the differential diagnosis of congenital hyperinsulinism. J Clin Endocrinol Metab 87:4502–4507
15. **Tornovsky S, Crane A, Cosgrove KE, Hussain K, Lavie J, Heyman M, Nesher Y, Kuchinski N, Ben-Shushan E, Shatz O, Nahari E, Potikha T, Zangen D, Tenenbaum-Rakover Y, de Vries L, Argente J, Gracia R, Landau H, Eliakim A, Lindley K, Dunne MJ, Aguilar-Bryan L, Glaser B** 2004 Hyperinsulinism of infancy: novel *ABCC8* and *KCNJ11* mutations and evidence for additional locus heterogeneity. J Clin Endocrinol Metab 89:6224–6234
16. **Henwood MJ, Kelly A, Macmullen C, Bhatia P, Ganguly A, Thornton PS, Stanley CA** 2005 Genotype-phenotype correlations in children with congenital hyperinsulinism due to recessive mutations of the triphosphate-sensitive potassium channel genes. J Clin Endocrinol Metab 90:789–794
17. **Crane A, Aguilar-Bryan L** 2004 Assembly, maturation, and turnover of K(ATP) channel subunits. J Biol Chem 279:9080–9090
18. **Tanizawa Y, Matsuda K, Matsuo M, Ohta Y, Ochi N, Adachi M, Koga M, Mizuno S, Kajita M, Tanaka Y, Tachibana K, Inoue H, Furukawa S, Amachi T, Ueda K, Oka Y** 2000 Genetic analysis of Japanese patients with persistent hyperinsulinemic hypoglycemia of infancy: nucleotide-binding fold-2 mutation impairs cooperative binding of adenine nucleotides to sulfonylurea receptor 1. Diabetes 49:114–120
19. **Graham FL, van der Eb AJ** 1973 A new technique for the assay of infectivity of human adenovirus 5 DNA. Virology 52:456–467
20. **Paulhe F, Imhof BA, Wehrle-Haller B** 2004 A specific endoplasmic reticulum export signal drives transport of stem cell factor (Kitl) to the cell surface. J Biol Chem 279:55545–55555
21. **Bloc A, Cens T, Cruz H, Dunant Y** 2000 Zinc-induced changes in ionic currents of clonal rat pancreatic β-cells: activation of ATP-sensitive K^+ channels. J Physiol 529:723–734
22. **Partridge CJ, Beech DJ, Sivaprasadarao A** 2001 Identification and pharmacological correction of a membrane trafficking defect associated with a mutation in the sulfonylurea receptor causing familial hyperinsulinism. J Biol Chem 276:35947–35952
23. **Cosgrove KE, Shepherd RM, Fernandez EM, Natarajan A, Lindley KJ, Aynsley-Green A, Dunne MJ** 2004 Genetics and pathophysiology of hyperinsulinism in infancy. Horm Res 61:270–288
24. **Zerangue N, Schwappach B, Jan YN, Jan LY** 1999 A new ER trafficking signal regulates the subunit stoichiometry of plasma membrane K(ATP) channels. Neuron 22:537–548
25. **Taschenberger G, Mougey A, Shen S, Lester LB, LaFranchi S, Shyng SL** 2002 Identification of a familial hyperinsulinism-causing mutation in the sulfonylurea receptor 1 that prevents normal trafficking and function of KATP channels. J Biol Chem 277:17139–17146
26. **Murshid A, Presley JF** 2004 ER-to-Golgi transport and cytoskeletal interactions in animal cells. Cell Mol Life Sci 61:133–145
27. **Tucker SJ, Gribble FM, Zhao C, Trapp S, Ashcroft FM** 1997 Truncation of Kir6.2 produces ATP-sensitive K^+ channels in the absence of the sulphonylurea receptor. Nature 387:179–183
28. **Yuan H, Michelsen K, Schwappach B** 2003 14-3-3 dimers probe the assembly status of multimeric membrane proteins. Curr Biol 13:638–646
29. **Cartier EA, Conti LR, Vandenberg CA, Shyng SL** 2001 Defective trafficking and function of KATP channels caused by a sulfonylurea receptor 1 mutation associated with persistent hyperinsulinemic hypoglycemia of infancy. Proc Natl Acad Sci USA 98:2882–2887
30. **Schonau E, Deeg KH, Huemmer HP, Akcetin YZ, Bohles HJ** 1991 Pancreatic growth and function following surgical treatment of nesidioblastosis in infancy. Eur J Pediatr 150:550–553
31. **Trucco M** 2005 Regeneration of the pancreatic β-cell. J Clin Invest 115:5–12
32. **Inagaki N, Gonoi T, Clement JP, Wang CZ, Aguilar-Bryan L, Bryan J, Seino S** 1996 A family of sulfonylurea receptors determines the pharmacological properties of ATP-sensitive K^+ channels. Neuron 16:1011–1017
33. **Inagaki N, Gonoi T, Clement 4th JP, Namba N, Inazawa J, Gonzalez G, Aguilar-Bryan L, Seino S, Bryan J** 1995 Reconstitution of IKATP: an inward rectifier subunit plus the sulfonylurea receptor. Science 270:1166–1170
34. **Isomoto S, Kondo C, Yamada M, Matsumoto S, Higashiguchi O, Horio Y, Matsuzawa Y, Kurachi Y** 1996 A novel sulfonylurea receptor forms with BIR (Kir6.2) a smooth muscle type ATP-sensitive K^+ channel. J Biol Chem 271: 24321–24324
35. **Sakura H, Ammala C, Smith PA, Gribble FM, Ashcroft FM** 1995 Cloning and functional expression of the cDNA encoding a novel ATP-sensitive potassium channel subunit expressed in pancreatic β-cells, brain, heart and skeletal muscle. FEBS Lett 377:338–344
36. **Seino S** 2003 Physiology and pathophysiology of K(ATP) channels in the pancreas and cardiovascular system: a review. J Diabetes Complications 17:2–5
37. **Thomzig A, Laube G, Pruss H, Veh RW** 2005 Pore-forming subunits of K-ATP channels, Kir6.1 and Kir6.2, display prominent differences in regional and cellular distribution in the rat brain. J Comp Neurol 484:313–330

European Journal of Endocrinology (2005) 153 167–176 ISSN 0804-4643

EXPERIMENTAL STUDY

Endoplasmic reticulum stress induces *Wfs1* gene expression in pancreatic β-cells via transcriptional activation

Kohei Ueda[1], June Kawano[2], Komei Takeda[3], Toshiaki Yujiri[3], Katsuya Tanabe[3], Takatoshi Anno[3], Masaru Akiyama[3], Junichi Nozaki[4], Takeo Yoshinaga[4], Akio Koizumi[4], Koh Shinoda[2], Yoshitomo Oka[5] and Yukio Tanizawa[3]

[1]*Health Service Center, Organization for University Education, Yamaguchi University,* [2]*Division of Neuroanatomy, Department of Neuroscience, and* [3]*Division of Molecular Analysis of Human Disorders, Department of Bio-Signal Analysis, Yamaguchi University Graduate School of Medicine, 1-1-1 Minami Kogushi, Ube, Yamaguchi 755-8505, Japan,* [4]*Department of Health and Environmental Sciences, Kyoto University Graduate School of Medicine, Kyoto, Japan, and* [5]*Division of Molecular Metabolism and Diabetes, Department of Internal Medicine, Tohoku University Graduate School of Medicine, Sendai, Japan*

(Correspondence should be addressed to Y Tanizawa; Email: tanizawa@yamaguchi-u.ac.jp)

Abstract

Objective: The *WFS1* gene encodes an endoplasmic reticulum (ER) membrane-embedded protein. Homozygous *WFS1* gene mutations cause Wolfram syndrome, characterized by insulin-deficient diabetes mellitus and optic atropy. Pancreatic β-cells are selectively lost from the patient's islets. ER localization suggests that WFS1 protein has physiological functions in membrane trafficking, secretion, processing and/or regulation of ER calcium homeostasis. Disturbances or overloading of these functions induces ER stress responses, including apoptosis. We speculated that WFS1 protein might be involved in these ER stress responses.

Design and methods: Islet expression of the Wfs1 protein was analyzed immunohistochemically. Induction of Wfs1 upon ER stress was examined by Northern and Western blot analyses using three different models: human skin fibroblasts, mouse pancreatic β-cell-derived MIN6 cells, and Akita mouse-derived *Ins2* $^{96Y/Y}$ insulinoma cells. The human *WFS1* gene promoter-luciferase reporter analysis was also conducted.

Result: Islet β-cells were the major site of *Wfs1* expression. This expression was also found in δ-cells, but not in α-cells. *WFS1* expression was transcriptionally up-regulated by ER stress-inducing chemical insults. Treatment of fibroblasts and MIN6 cells with thapsigargin or tunicamycin increased *WFS1* mRNA. WFS1 protein also increased in response to thapsigargin treatment in these cells. *WFS1* gene expression was also increased in *Ins2* $^{96Y/Y}$ insulinoma cells. In these cells, ER stress was intrinsically induced by mutant insulin expression. The *WFS1* gene promoter-luciferase reporter system revealed that the human *WFS1* promoter was activated by chemically induced ER stress in MIN6 cells, and that the promoter was more active in *Ins2* $^{96Y/Y}$ cells than *Ins2* $^{wild/wild}$ cells.

Conclusion: *Wfs1* expression, which is localized to β- and δ-cells in pancreatic islets, increases in response to ER stress, suggesting a functional link between *Wfs1* and ER stress.

European Journal of Endocrinology **153** 167–176

Introduction

Wolfram syndrome is a rare recessively inherited genetic disorder, which is characteristically associated with juvenile onset diabetes mellitus and progressive optic atropy (1). Sensorineural deafness, diabetes insipidus, ataxia, urinary-tract atony, peripheral neuropathy and psychiatric illness may also be present (2). We and another group succeeded in cloning the gene responsible for this disorder and designated it *WFS1* (3) or *wolframin* (4). Loss-of-function mutations in the *WFS1* gene have been linked to Wolfram syndrome. The *WFS1* gene consists of eight exons coding for a putative 890 amino acid protein with an apparent molecular mass of ~100 kDa. WFS1 protein (wolframin) is a hydrophobic protein with nine transmembrane segments and large hydrophilic regions at both termini. WFS1 protein localizes primarily to the endoplasmic reticulum (ER) in a N_{cyt}/C_{lum} membrane topology (5, 6). A recent report suggested that expression of WFS1 protein in oocytes was associated with an increase in cytosolic Ca^{2+} and induced novel cation-selective channel activities in the ER membrane (7). However, its role in cellular functions and the mechanism by which mutations of this gene cause Wolfram syndrome remain largely unknown.

DOI: 10.1530/eje.1.01945
Online version via www.eje-online.org

ER is a specialized organella involved in a wide variety of cellular functions. Calcium regulation and post-translational modification, folding and trafficking of secreted and membrane integral proteins are well-defined ER functions (8). Various physiological and pathological conditions interfere with these functions, and overloading of these functions induces ER stress. Cells respond to such stress by activating several adaptive pathways including chaperone induction, protein translation attenuation, and occasionally apoptosis, collectively called the unfolded protein response (9). Characteristically, pancreatic β-cells have highly developed ER apparently due to the heavy demands of insulin biosynthesis and secretion. Beta-cells are highly susceptible to ER stress. Several studies have shown that β-cell mass is reduced in patients with type 2 diabetes, possibly due to apoptotic death of β-cells and to reduced cell proliferation (10). ER stress may be involved in this process (11). In the Akita mouse, an animal model of MODY (maturity onset diabetes of the young), which carries a conformation-altering missense mutation (Cys96Tyr) in the insulin-2 (*Ins2*) gene (12, 13), hyperglycemia and reduced β-cell mass are accompanied by ER stress-induced β-cell death (14). Based on the ER localization of WFS1 protein, it is reasonable to speculate that WFS1 protein may play an as yet undefined role in the ER stress-induced cell death of pancreatic β-cells. In fact, we showed islet cells lacking Wfs1 to be more susceptible to ER stress-induced apoptosis (15), and, more recently, Yamaguchi *et al.* reported that treatment with ER stress inducers increased Wfs1 protein expression in isolated mouse pancreatic islets (16).

In the present study, immunohistochemical staining confirmed β-cells to be the major site of *Wfs1* expression in the mouse pancreas. Furthermore, this expression was also evident in δ-cells but not in α-cells. The *WFS1* gene was clearly expressed in response to drug-induced ER stress in both fibroblasts and pancreatic β-cell-derived MIN6 cells. Under the same conditions, the human *WFS1* promoter luciferase reporter was activated suggesting transcriptional control of *WFS1* expression. Furthermore, *Wfs1* mRNA and protein levels were increased in Akita mouse-derived *Ins2* $^{96Y/Y}$ insulinoma cells, in which the ER stress response had been triggered (17). Our results demonstrate that not only drug-induced but also intrinsic ER stress leads to *WFS1* expression in pancreatic β-cells, and this occurs, at least in part, via transcriptional activation of the *WFS1* promoter. These findings further suggest a functional link between *WFS1* and ER stress responses.

Research design and methods

Tissue preparation and immunohistochemical staining of the mouse pancreas

All experimental protocols for this study were approved by the committee on the Ethics of Animal Experimentation at Yamaguchi University School of Medicine. The anti-Wfs1 antibodies were described previously (5, 15).

Double immunofluorescent staining was performed for co-localization studies. Sections were pre-incubated, bleached (18), and stained with a mixture of anti-Wfs1n (diluted 1:200) and mouse monoclonal anti-insulin (diluted 1:100; Santa Cruz Biotechnology, Santa Cruz, CA, USA), anti-glucagon (diluted 1:200; Sigma-Aldrich, St Louis, MO, USA), or anti-somatostatin (diluted 1:25; Biomeda Corporation, Foster City, CA, USA) in 0.1 M sodium phosphate buffer containing 0.3% Triton X-100, 0.1% sodium azide, and 3% normal goat serum (PBT-NGS) for 24 h at 20 °C. Next, the sections were incubated with a mixture of two secondary antibodies in PBT-NGS for 24 h at 20 °C. The secondary antibodies used were Alexa Fluor 488 conjugated with goat anti-rabbit IgG (H + L), highly cross absorbed (Molecular Probes, Eugene, OR, USA) and diluted 1:100, and an Alexa Fluor 594 conjugated to goat anti-mouse IgG (H + L), F(ab')2 fragment (Molecular Probes), diluted 1:100. The sections were coverslipped with VECTASHIELD mounting medium (Vector Laboratories, Burlingame, CA, USA). As a control, one of the two primary antibodies, for example either anti-Wfs1n or anti-insulin, was removed to check for cross-reactivity. In these control experiments, other procedures were the same as for Wfs1/insulin double staining. No cross-reactivity was observed in these experiments (data not shown).

In the case of double immunostaining for Wfs1 and pancreatic polypeptide (PP) detection, a mixture of anti-Wfs1n (diluted 1:200) and anti-PP (diluted 1:200; Linco Research, St Charles, MO, USA) was used for the primary antibody reaction. In the secondary antibody reaction step, sections were incubated in a mixture of Alexa Fluor 488 conjugated with donkey anti-rabbit IgG (H + L; Molecular Probes) diluted 1:100 and Alexa Fluor 594 conjugated to goat anti-guinea pig IgG (H + L), highly cross absorbed (Molecular Probes) and diluted 1:100 in PBT-NGS containing 3% normal donkey serum. Other procedures for Wfs1/PP double staining were the same as for Wfs1/insulin double staining.

Cell culture and reagents

The mouse insulinoma cell line, MIN6 (19), was a gift from Dr Junichi Miyazaki, Osaka University, Japan. Insulinoma cells derived from the Akita mouse and from normal littermates, *Ins2* $^{96Y/Y}$ cells and *Ins2* $^{WT/WT}$ cells respectively, were described previously (17). These cells were maintained in Dulbecco's modified Eagle's medium (DMEM) (Sigma) supplemented with 15% fetal calf serum in an atmosphere of 5% CO_2 at 37 °C. The genotype for the insulin-2 gene was confirmed by restriction fragment length polymorphism (RFLP), as previously described (12, 13). Human skin fibroblasts

(CCD-1059SK) were obtained from ATCC (Manassas, VA, USA). Thapsigargin, ionomycin, A23187, cyclopiazonic acid, 4-chloro-*m*-cresol, tunicamycin and brefeldin A were purchased from Sigma.

Northern blot analysis

Total RNA isolated using an ISOGEN kit (NIPPON GENE, Tokyo, Japan) was electrophoresed in 1% agarose formaldehyde gel and transferred to nylon filters (Hybond-N plus, Amersham Pharmacia Biotech). The filters were prehybridized and hybridized in a buffer containing 50% deionized formamide, 5 × sodium chloride-sodium phosphate-EDTA buffer (750 mmol/l NaCl, 43.25 mmol/l NaH_2PO_4, 6.25 mmol/l EDTA), 2 × Denhardt's solution (0.04% bovine serum albumin, 0.04% Ficoll, 0.04% polyvinylpyrrolidone), and 0.1% soduim dodecyl sulfate at 42 °C. The hybridization buffer contained a radio-labeled 3.0 kb fragment of mouse *Wfs1* cDNA (GeneBank Accession No. BC046988). After a stringent wash with 0.2 × sodium chloride-sodium citrate buffer (3.3 mmol/l Na-citrate, 3.3 mmol/l NaCl) and 0.1% SDS at 50 °C, autoradiographs were digitally scanned and quantified using FULA2000 (Fuji Film, Tokyo, Japan). The blots were stripped and re-proved with a 1122 bp fragment encompassing the entire coding region of the mouse glyceraldehyde-3-phosphate dehydrogenase (GAPDH) cDNA. The cDNA probes were labeled with a random primer DNA labeling kit (Ready-To-Go DNA Labeling Beads, Amersham Pharmacia Biotech) using α-[^{32}P]deoxy-CTP (Amersham Pharmacia Biotech).

Immunoblotting analysis

Cells were lysed in 20 mmol/l Tris–HCl (pH 7.6), 0.5% Nonidet P-40, 250 mmol/l sodium chloride, 3 mmol/l EDTA, 3 mmol/l EGTA, 1 mmol/l phenylmethylsulfonyl fluoride, 2 mmol/l sodium orthovanadate, 20 μg/ml aprotinin, 1 mmol/l dithiothreitol and 5 μg/ml leupeptin. Proteins in cell lysates were separated in 10% SDS-PAGE gel and then electrophoretically transferred onto a nitrocellulose membrane. All membranes were stained with Ponceau S to confirm equal protein loading. The membrane was blocked with 5% milk in TBS-T (50 mmol/l Tris–HCl, 300 mmol/l NaCl, pH 7.6, 0.1% Tween 20) for 1 h. SDS-PAGE and immunoblotting were carried out as described previously (20). Anti-Bip (GRP74), anti-Chop, anti-phosphorylated eIF2-α, and anti-poly(ADP-ribose) polymerase (PARP) antibodies were purchased from Santa Cruz Biotechnology. Detection was performed using the ECL system (Amersham Pharmacia Biotech).

Luciferase assay

To construct the *WFS1* promoter-luciferase reporter gene, the promoter region of the human *WFS1* gene (−3000 to +20, Genbank Accession No. AC004689) was PCR-amplified from human genomic DNA. The fragment was inserted upstream from the luciferase cDNA in a pGL3-Basic vector (Promega, Madison, WI, USA). A plasmid, pCMVβ (Clontech, Palo Alto, CA, USA), containing the cytomegalovirus (CMV) promoter-driven β-galactosidase gene was used as an internal control for the normalization of transfection efficiency. One day before transfection, MIN6 cells or *Ins2* $^{96Y/Y}$ cells were plated at 1×10^5/well into 6-well tissue culture plates. The reporter plasmid (0.5 μg) and the pCMVβ (0.5 μg) were co-transfected into MIN6 cells or *Ins2* $^{96Y/Y}$ cells in 6-well tissue culture plates using 10 μl LipofectAMINE 2000 (Invitrogen) in serum-free Opti-MEM medium (Invitrogen). Twenty-four hours after transfection, the medium was changed to DMEM containing 15% fetal calf serum and 20 mmol/l glucose, and cultured for a further 24 h. After this 24-h incubation, MIN6 cells were treated with thapsigargin or tunicamycin for an additional 6 h. Cell extracts were prepared, and luciferase and β-galactosidase activities were determined using a β-galactosidase enzyme assay system according to the manufacturer's protocol (Promega).

Results

Wfs1 *expression in the mouse pancreatic islet*

Using immunohistochemistry, it was demonstrated that mouse Wfs1 protein was widely expressed in pancreatic islets except in some peripheral areas, while no signals for Wfs1 protein were detected in exocrine acinar cells (Figs 1 and 2 and data not shown). Using double-immunofluorescent staining, the majority of Wfs1-immunoreactive cells were found to coincide with insulin-producing β-cells. Some minor part of the Wfs1 immunoreactivity was, however, localized to non-β-cells seen in the islet periphery (Fig. 1A–F). Such Wfs1-immunoreactive non-β-cells were found to correspond to somatostatin-producing δ-cells (Fig. 1G–L). There was little difference in Wfs1-immunoreactive intensity between the two endocrine cell types (Fig. 1). Wfs1-immunoreactivity was not evident in glucagon-producing α-cells or in pancreatic polypeptide cells (PP-cells; Fig. 2).

ER stress induces WFS1 *expression in fibroblasts*

ER stress induces cellular responses, collectively termed the unfolded protein response, affecting diverse areas of cellular function such as gene expression, metabolism, cell signaling and apoptosis. Certain reagents are known to disturb ER calcium homeostasis or to inhibit post-translational processing or sorting, and thereby to cause ER stress (9). Chemical insults inducing ER stress, the calcium ionophor A23187 and ionomycin,

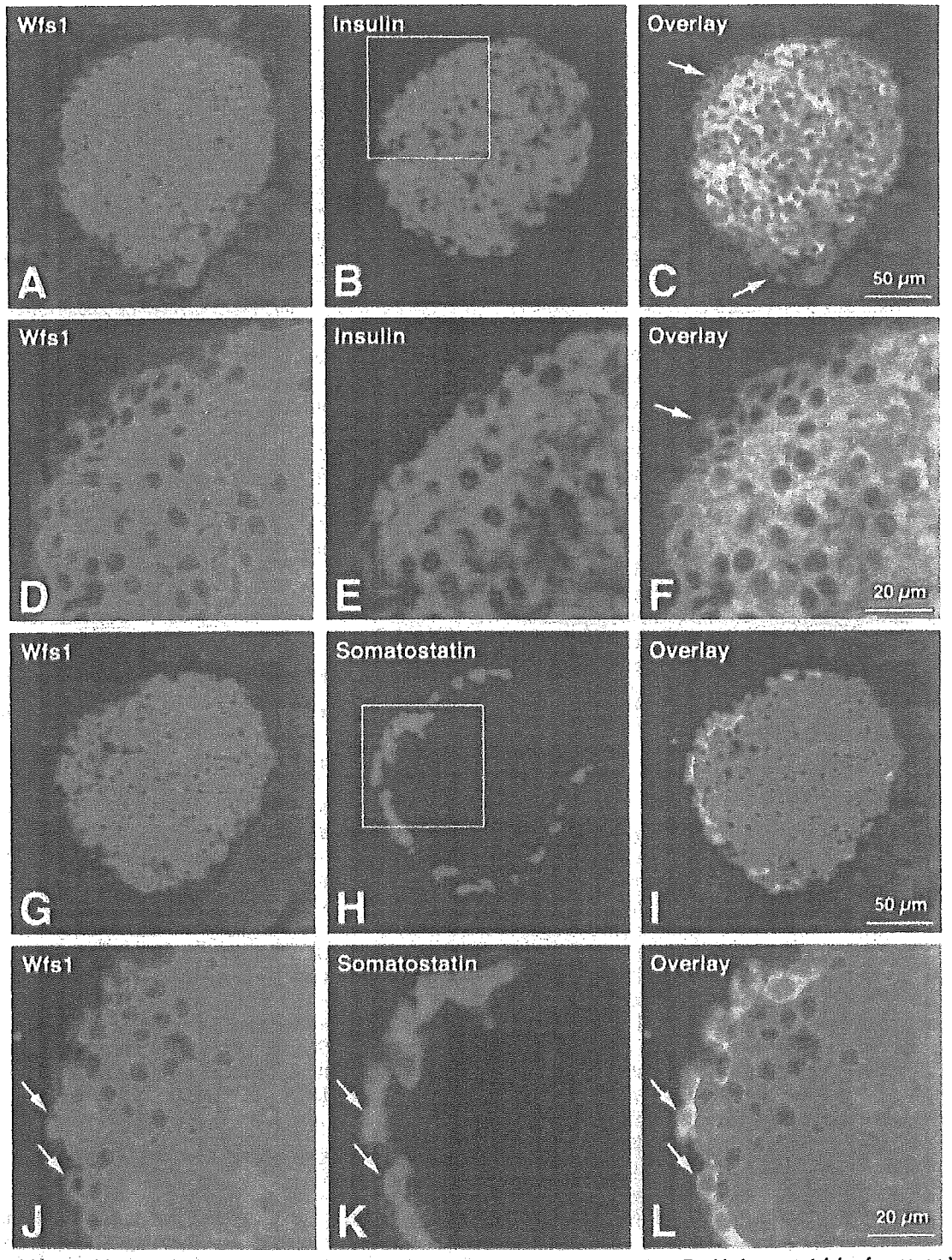

Figure 1 Mouse Wfs1 protein, insulin and somatostatin expression in mouse pancreatic islets. Double immunostaining for mouse Wfs1 (Wfs1: A, D, G, J; Alexa Fluor 488 label; green) and pancreatic hormones (insulin: B, E; somatostatin: H, K; Alexa Fluor 594 label; red) was performed. Panels C, F, I and L are overlaid images. All fluorescent photomicrographs were taken with a confocal microscope LSM 510 (Carl Zeiss Jena GmbH, Jena, Germany). The approximate positions of E and K are indicated by the rectangular frames in B and H respectively. Small solid arrows in C and F indicate non-β endocrine cells immunoreactive for Wfs1. Small solid arrows in J, K and L show somatostatin-producing δ-cells strongly immunoreactive for Wfs1. Note that insulin-producing β-cells and somatostatin-producing δ-cells display Wfs1 immunoreactivity. Scale bars = 50 μm in C and I for A, B, and for G, H; 20 μm in F and L for D, E, and for J, K.

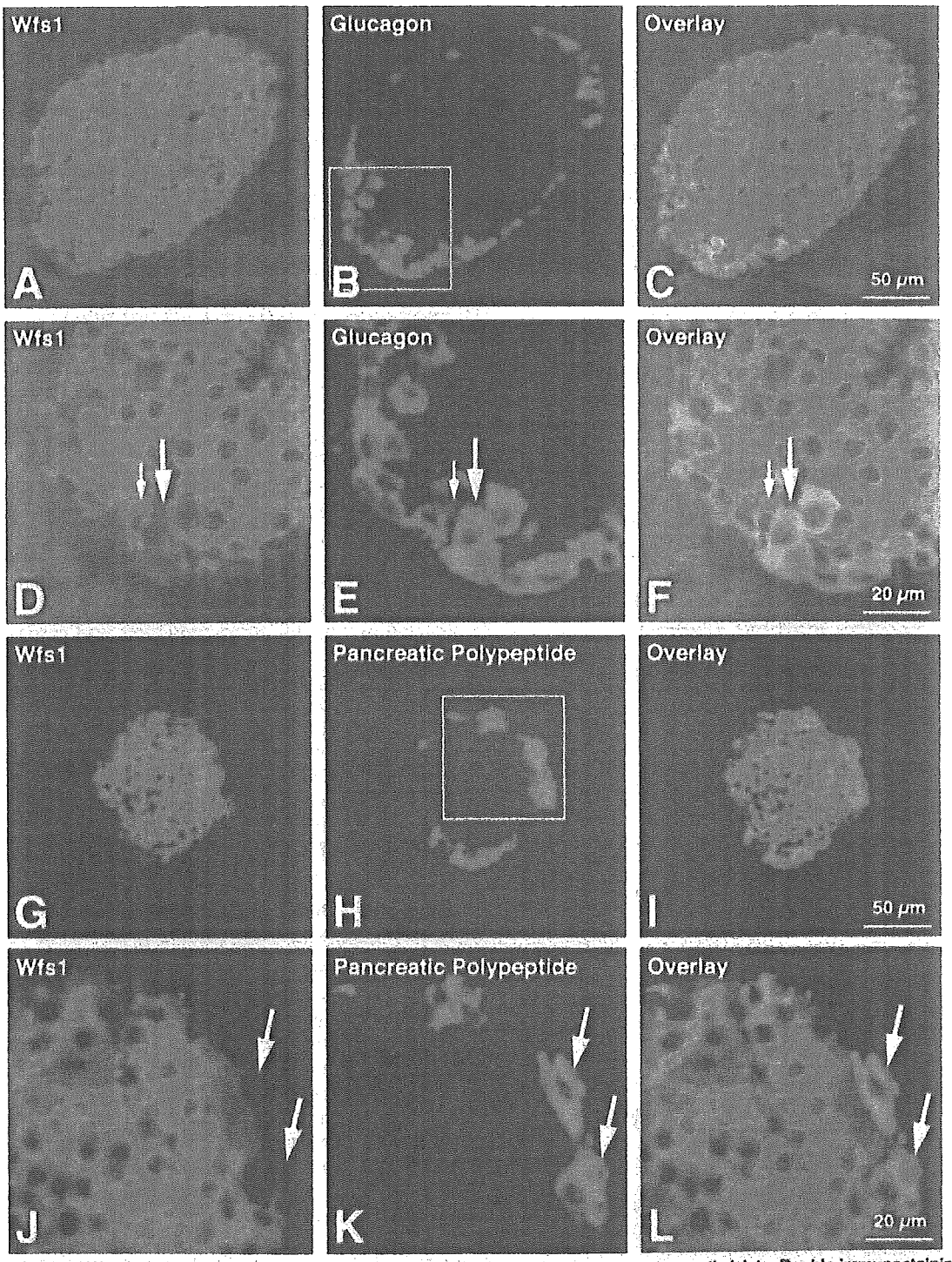

Figure 2 Mouse Wfs1 protein, glucagon and pancreatic polypeptide expression in mouse pancreatic islets. Double immunostaining for mouse Wfs1 (Wfs1: A, D, G, J; Alexa Fluor 488 label; green) and pancreatic hormones (glucagon: B, E; pancreatic polypeptide: H, K; Alexa Fluor 594 label; red) was performed. Panels C, F, I and L are overlaid images. All fluorescent photomicrographs were taken with a confocal microscope LSM 510 (Carl Zeiss Jena GmbH). The approximate positions of E and K are indicated by the rectangular frames in B and H respectively. Large and small solid arrows in D, E and F indicate glucagon-producing α-cells negative for Wfs1 immunoreactivity and non-α endocrine cells positive for Wfs1 immunoreactivity respectively. Large solid arrows in J, K and L show pancreatic polypeptide cells (PP-cells) negative for Wfs1 immunoreactivity. Scale bars = 50 μm in C and I for A, B, and for G, H; 20 μm in F and L for D, E, and for J, K.

the ER Ca^{2+}-ATPase inhibitors (21) thapsigargin and cyclopiazonic acid, the ryanodine receptor activator 4-chloro-*m*-cresol, and the protein *N*-glycosylation inhibitor tunicamycin all induced WFS1 protein as shown in Fig. 3. Only brefeldin A had no effect. Ionomycin only weakly induced WFS1 protein. The differing effects of these chemicals, which have different mechanisms of action, may provide insights into the functions of Wfs1. The lack of WFS1 induction with brefeldin A, a Golgi apparatus disruptor, may be related to its instability in solution (22). Although we did not perform Northern blot analysis for each of these reagents, A23187 induced *WFS1* mRNA in fibroblasts (data not shown).

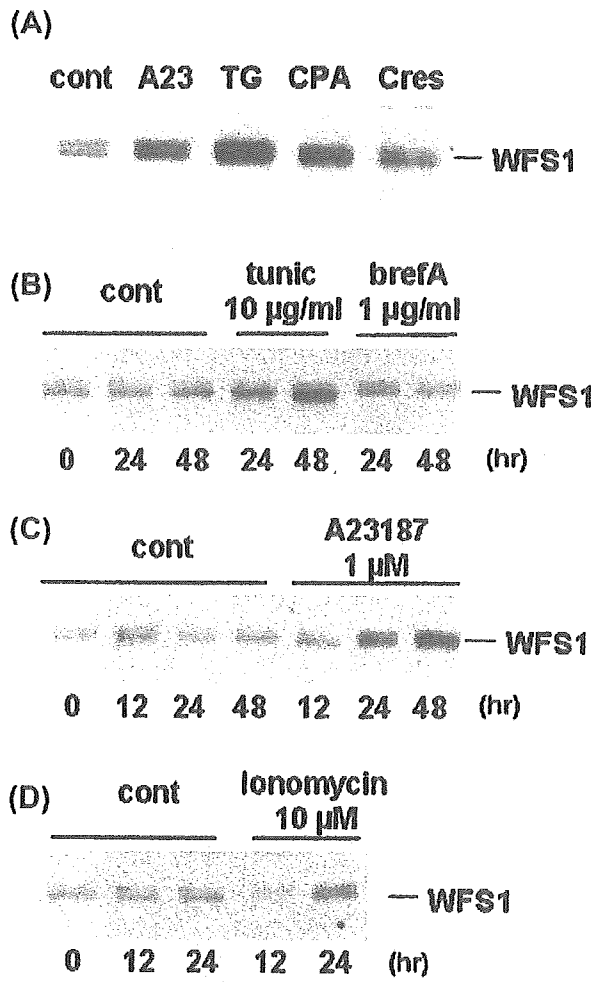

Figure 3 ER stress induces WFS1 protein in fibroblasts. Primary skin fibroblasts were cultured in the presence of (A) A23187 (A23, 1 μmol/l), thapsigargin (TG, 1 μmol/l), cyclopiazonic acid (CPA, 10 μmol/l) and 4-chloro-*m*-cresol (cres, 50 μmol/l) for 48 h. (B–D) Cells were treated for the indicated time periods with (B) tunicamycin (tunic), brefeldin A (brefA), (C) A23187, and (D) ionomycin. cont indicates control. Control samples included a vehicle (DMSO), also administered with all of the drugs. Cells were harvested after the incubation periods, and total cell lysates containing 20 μg protein were subjected to Western blot analysis using anti-WFS1c antibody.

Effects of thapsigargin and tunicamycin on Wfs1 *expression in MIN6 cells*

We next examined the effects of thapsigargin and tunicamycin on the expression of *Wfs1* mRNA in MIN6 cells. Thapsigargin and tunicamycin treatments are known to induce ER stress, and Chop/GADD153 is a transcription factor that plays a role in ER stress-induced apoptotic cell death (23, 24). Phosphorylation of the α-subunit of translation initiation factor-2 (eIF2-α) attenuates protein translation upon ER stress. Although the ER chaperone Bip/GRP78 expression did not change in MIN6 cells (Fig. 4B) probably due to its strong basal expression, thapsigargin and tunicamycin clearly generated ER stress as demonstrated by Chop induction and eIF2-α phosphorylation (Fig. 4A, B). Under these conditions, ER stress-induced caspase-3 activation, an event at the initiation of apoptosis (25), was evidenced by the cleavage of PARP (Fig. 4C). PARP is one of the substrates cleaved by caspase-3. Upon thapsigargin or tunicamycin treatment, the 113 kDa band decreased, and instead, the proteolytic PARP fragment (89 kDa) appeared (Fig. 4C). In association with ER stress induction and caspase-3 activation, *Wfs1* mRNA expression increased (Fig. 4A,D). With thapsigargin, *Wfs1* mRNA started to increase after 6 h and was maximal after 12 h. With tunicamycin, *Wfs1* mRNA induction peaked at 6 h, and then declined. Wfs1 protein was also increased by thapsigargin treatment (Fig. 4B). In contrast, tunicamycin, despite the mRNA induction, did not increase the Wfs1 protein, but decreased it after 24 h (Fig. 4B). This is probably due to the instability of unglycosylated Wfs1 protein (6, 16).

Thapsigargin and tunicamycin enhance human WFS1 *promoter activity in MIN6 cells*

To determine the mechanism of *WFS1* expression, we examined the effects of thapsigargin and tunicamycin on human *WFS1* gene promoter activity by employing transient transfection assays in MIN6 cells. We used a *WFS1* promoter-luciferase construct that contained a 3 kb DNA sequence upstream from the human *WFS1* gene transcription initiation site. The human *WFS1* gene promoter was active in MIN6 cells. Introduction of the *WFS1* promoter-reporter plasmid produced a 20-fold increase in luciferase activity as compared with the promoterless pGL3-Basic vector. Treatment of the cells with thapsigargin or tunicamycin resulted in further 1.3- and 1.5-fold increases in luciferase activity respectively (Fig. 5). We conducted these experiments again using a 1 kb (−1000 to +20) *WFS1* promoter-luciferase reporter gene. The results were essentially the same but the promoter activity was weaker than with the 3 kb construct (data not shown).

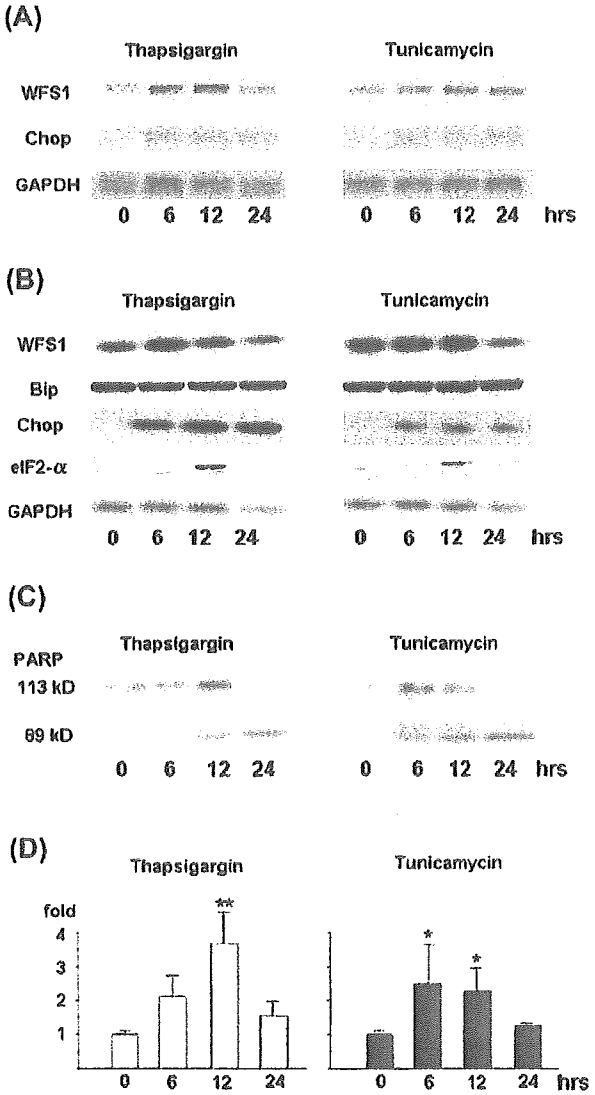

Figure 4 Thapsigargin and tunicamycin increase *Wfs1* mRNA expression in MIN6 cells in association with ER stress and apoptosis induction. MIN6 cells were placed in culture dishes and serum-starved in serum-free DMEM for 12 h, and then treated with thapsigargin (1 μmol/l) or tunicamycin (10 μg/ml) for 6, 12 or 24 h. Dimethyl sulfoxide (DMSO) was used to dissolve thapsigargin and tunicamycin, and the same concentration of DMSO (final, 0.05%) was employed in all experiments, including controls. After incubation, cells were washed once with ice-cold phosphate-buffered saline, and harvested. (A) Ten micrograms RNA were subjected to Northern blot analysis. (B) Total cell lysates containing equal amounts of protein (50 μg) were separated on 10% SDS-PAGE and analyzed by immunoblotting using anti-Wfs1n, anti-Bip (GRP74), anti-Chop or anti-phosphorylated eIF2-α, (C) Total cell lysates containing equal amounts of protein (50 μg) were separated on 10% SDS-PAGE and analyzed by immunoblotting using the anti-PARP antibody. Activated caspase-3 cleaves the 113 kDa PARP, resulting in the appearance of the 89 kDa fragment. (D) Quantification of the *Wfs1* mRNA from the results obtained in (A), shown as means±S.E. ($n = 4$). Statistical analysis, conducted using analysis of variance, indicated that the thapsigargin and tunicamycin treatments significantly increased *Wfs1* mRNA expression at 12 h and at 6 h and 12 h respectively (*$P < 0.05$, **$P < 0.001$).

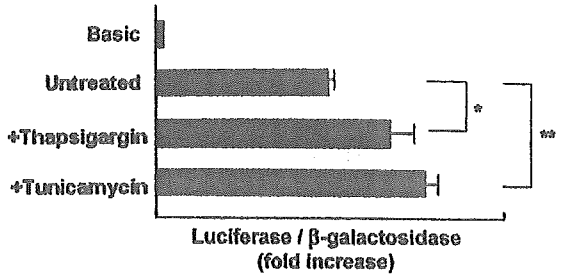

Figure 5 ER stress enhances *WFS1* promoter activity in MIN6 cells. MIN6 cells were transfected with a luciferase reporter plasmid containing a 3.0 kb human *WFS1* gene 5' flanking promoter region (from −3000 to +20) and were exposed to thapsigargin (1 μmol/l) or tunicamycin (10 μg/ml) for 6 h. Beta-galactosidase activity from the co-transfected expression vector pCMVβ was used to calibrate for transfection efficiency. Basic represents luciferase activity from pGL3-Basic (promoterless) vector-transfected cells. Results are expressed as the fold increase as compared with basic (means±S.E. of four independent experiments, each performed in triplicate). *P* values for comparison of results with versus without drug treatments are 0.034 (thapsigargin, *) and 0.005 (tunicamycin, **) (analysis of variance).

Wfs1 *expression is transcriptionally upregulated in β-cells with intrinsic ER stress*

In the Akita mouse, the C96Y mutation of the *ins2* gene disturbs intramolecular disulfide bond formation, resulting in progressive β-cell loss (12). ER stress and subsequent apoptosis are at least partially responsible for this progressive β-cell loss (14). To further examine the association between increased *Wfs1* expression and ER stress, we used mouse insulinoma cells derived from an Akita mouse homozygous for the *ins2* gene C96Y mutation (*Ins2* $^{96Y/Y}$ cell) as a model. *Ins2* $^{WT/WT}$ cells derived from normal littermates served as controls. Doubling of the ER chaperone Bip/GRP78 in *Ins2* $^{96Y/Y}$ cells indicated persistent ER stress in these cells (Fig. 6A). In Ins2$^{96Y/Y}$ cells, Wfs1 protein increased sixfold as compared with that in *Ins2* $^{WT/WT}$ cells (Fig. 6B). *Wfs1* mRNA expression was also increased twofold (data not shown). We next examined *WFS1* promoter activity in these cells. Introduction of the *WFS1* promoter-reporter plasmid into *Ins2* $^{96Y/Y}$ cells approximately doubled luciferase activity as compared with that in wild type *Ins2* $^{WT/WT}$ cells (Fig. 7). Luciferase activity after transfection of the SV40 promoter-reporter plasmid did not differ between *Ins2* $^{96Y/Y}$ and *Ins2* $^{WT/WT}$ cells.

Discussion

Herein, we have documented the localization of Wfs1 expression in the mouse pancreatic islet. Insulin-producing β-cells are the major site of Wfs1 expression, as shown in Ishihara *et al.* (15). Wfs1 expression is also evident in somatostatin-producing δ-cells, but is absent from glucagon producing α-cells and PP-cells. No *Wfs1* expression is observed in pancreatic exocrine acinar

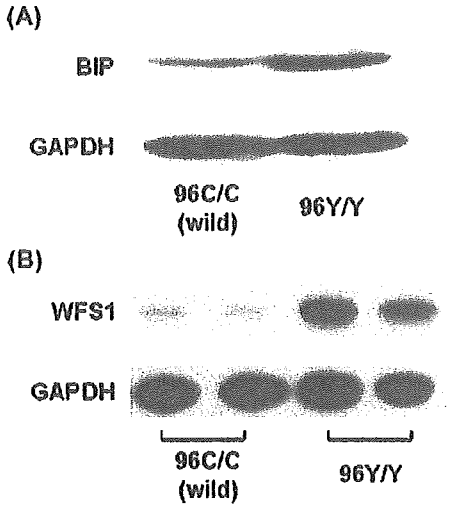

Figure 6 *WFS1* expression is increased in Akita mouse-derived *Ins2*$^{96Y/Y}$ cells. Cell extracts of *Ins2*$^{96Y/Y}$ cells containing equal amounts of protein (50 μg) were separated on 10% SDS-PAGE and analyzed by immunoblotting using (A) anti-Bip, and (B) anti-WFS1n and anti-GAPDH antibodies. Insulinoma cells derived from wild type littermates (wild) were used as the control. In (B), cell extracts were prepared on two separate occasions from cells derived from the same mutant mouse.

cells. A histopathological study of pancreatic islets from Wolfram syndrome patients showed selective loss of insulin-producing β-cells and an apparent preservation of glucagon-producing α-, somatostatin-producing δ-, and PP-cells (26, 27). The histochemical evidence of Wfs1 protein localization in insulin-producing β-cells might provide a histological background explaining the insulin deficiency caused by *WFS1* mutations in Wolfram syndrome patients and suggests that WFS1 protein is necessary for β-cell (28, 29), but not δ-cell survival.

We have also presented evidence herein that ER stress induces *Wfs1* gene expression. Treatment of fibroblasts with A23187, ionomycin, thapsigargin, cyclopiazonic acid, 4-chloro-*m*-cresol or tunicamycin increased *Wfs1* protein levels. Chemical insults by these reagents are known to induce ER stress via disruption of Ca^{2+} homeostasis or inhibition of N-linked glycosylation. Thapsigargin and tunicamycin treatments also induced *Wfs1* mRNA expression in a mouse β-cell line, MIN6 cells. In accordance with the mRNA change, thapsigargin increased Wfs1 protein expression. However, the Wfs1 protein level in MIN6 cells did not change with tunicamycin. This is probably due to Wfs1 being an N-glycosylated protein, and inhibition of glycosylation by tunicamycin decreases its stability (6, 16). Increased *Wfs1* expression in association with ER stress was further demonstrated in another β-cell model with ER stress: *Ins2*$^{96Y/Y}$ cells derived from the Akita mouse. The Akita mouse spontaneously develops early-onset non-obese diabetes with a reduced β-cell mass, which is caused by a conformation-altering missense mutation (Cys96Tyr) in the insulin-2 gene (12, 13). Intramolecular disulfide-bond formation is disrupted in the mutant insulin molecule. It was reported that this misfolded mutant insulin expression constitutively induced ER stress in Akita mouse β-cells (14). We have indeed confirmed increased Bip protein expression in *Ins2*$^{96Y/Y}$ cells as compared with wild type *Ins*$^{WT/WT}$ cells derived from normal littermates. In *Ins2*$^{96Y/Y}$ cells, *Wfs1* mRNA (data not shown) and protein levels (Fig. 6) were both increased. The increased *Wfs1* mRNA (twofold, data not shown) was consistent with the increased *Wfs1* promoter activity (Fig. 7). Our results provide further evidence, i.e. a detailed analysis, that *Wfs1* expression increases in association with ER stress, especially in the pancreatic β-cells selectively lost in patients with Wolfram syndrome. It is noteworthy that the increase in Wfs1 protein was marked (sixfold) as compared with the modest increase in Bip expression (twofold) in *Ins2*$^{96Y/Y}$ cells. Mechanisms other than ER stress might have further increased Wfs1 protein expression in this cell line.

The increase in *Wfs1* expression is attributable, at least in part, to enhanced *Wfs1* transcription, because both ER stress-inducing chemical insults (MIN6 cells) and intrinsic ER stress (*Ins2*$^{96Y/Y}$cells) stimulated *WFS1* promoter activity as demonstrated by a transient transfection assay using a human *WFS1* promoter-luciferase reporter construct. A cis-acting ER stress responsive element (ERSE) has been identified in the proximal promoter regions of chaperone-encoding genes. This element consists of a consensus sequence of

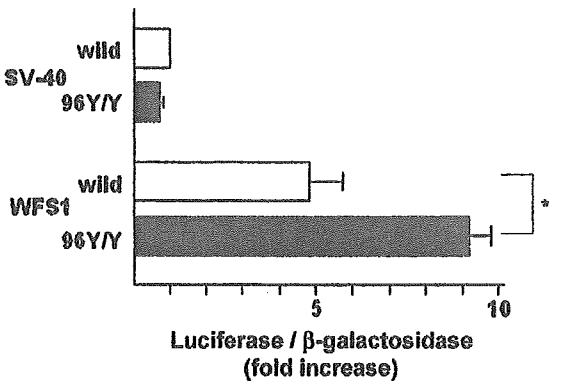

Figure 7 *WFS1* promoter activity is enhanced in *Ins2*$^{96Y/Y}$ cells. *Ins2*$^{96Y/Y}$ cells or wild type (wild) control cells were transfected with a luciferase reporter plasmid containing the 3.0 kb human *WFS1* gene 5′ flanking promoter region (from −3000 to +20), or a control plasmid containing the SV40 promoter-luciferase reporter. The expression vector pCMVβ was co-transfected, and β-galactosidase activity was used to calibrate for transfection efficiency. Results are expressed as fold-increases relative to luciferase/β-galactosidase activities in *Ins2*$^{96Y/Y}$cells as compared with control *Ins2*$^{WT/WT}$ cells in four independent experiments (means±S.E.), each performed in triplicate. *WFS1* promoter activity was significantly increased in *Ins2*$^{96Y/Y}$ cells as compared with control *Ins2*$^{WT/WT}$ cells (*$P = 0.014$, Student's *t*-tests).

CCAAT-N9-CCACG (30). The general transcriptional factor, NF-Y/CBF, binds to the CCAAT motif of the ERSE (31). Once ER stress ensues, p50ATF6 (active form of transcriptional factor ATF6) binds to the CCACG motif of the ERSE (31, 32) resulting in transcriptional induction of ER chaperones. Another ERSE (ERSE-II) with a consensus sequence of ATTGG-N-CCACG has also been identified (32). Although there are six CCAAT motifs in the −2800 to −2300 region of the putative human *WFS1* promoter, we found no ERSE consensus sequences within 3 kb upstream from the transcription initiation site. Further studies will be required to elucidate the mechanism of transcriptional regulation of the *Wfs1* gene via ER stress.

The observations made in this study suggest that Wfs1 protein may be involved in the ER stress response pathway, i.e. the unfolded protein response, in which cells respond by inducing chaperones, attenuating protein translation, and inducing apoptosis. Pancreatic β-cells suffer under chronic ER stress, striving to meet the increasing demands of insulin biosynthesis and secretion. In patients with Wolfram syndrome (26) and in *Wfs1* knock-out mice (15), β-cells were selectively lost from pancreatic islets. Moreover, islets from *Wfs* $^{-/-}$ mice were highly susceptible to ER stress (thapsigargin and tunicamycin)-induced apoptosis (15). It is tempting to speculate that Wfs1 protein is upregulated in response to ER stress and that it plays a physiological role in protecting cells from ER stress-induced apoptosis. Loss of function mutations of the *Wfs1* gene may cause β-cell loss due to disruption of this protective function. It was recently reported that Wfs1 protein expressed in oocytes exhibited a cation-selective ion channel activity (7). Expression of Wfs1 protein in oocytes increased cytosolic Ca^{2+} levels (7), and islets from *Wfs1* $^{-/-}$ mice exhibited attenuated glucose-stimulated intracellular Ca^{2+} responses (15). Wfs1 protein may be involved in the maintenance of ER and intracellular Ca^{2+} homeostasis, and its expression is induced under conditions of perturbed homeostasis, including ER stress.

The current findings that Wfs1 protein, which is predominantly expressed in pancreatic islet β-cells, is transcriptionally upregulated by ER stress indicate a link between Wfs1 protein function and ER stress responses. Further investigations utilizing *Wfs1* $^{-/-}$ mice and *Wfs1* $^{-/-}$ β-cells will provide insights into Wfs1 protein function and the pathophysiology of Wolfram syndrome.

Acknowledgements

We thank Professor Junichi Miyazaki, Osaka University, Japan, for providing us with MIN6 cells. This study was supported in part by Grants-in-Aid for Scientific Research (14370338 and 16390096 to Y Tanizawa) from the Ministry of Education, Culture, Sports, Science and Technology of Japan, grant no.15591228 (to J Kawano) from the Japan Society for Promotion of Science, and a grant from Takeda Science Foundation.

References

1 Barrett TG & Bundey SE. Wolfram (DIDMOAD) syndrome. *Journal of Medical Genetics* 1997 **34** 838–841.
2 Barrett TG, Bundey SE & Macleod AF. Neurodegeneration and diabetes: UK nationwide study of Wolfram (DIDMOAD) syndrome. *Lancet* 1995 **346** 1458–1463.
3 Inoue H, Tanizawa Y, Wasson J, Behn P, Kalidas K, Bernal-Mizrachi E, Mueckler M, Marshall H, Donis-Keller H, Crock P, Rogers D, Mihuni M, Kumashiro H, Higashi K, Sobue G, Oka Y & Permutt MA. A gene encoding a transmembrane protein is mutated in patients with diabetes mellitus and optic atrophy (Wolfram syndrome). *Nature Genetics* 1998 **20** 143–148.
4 Strom TM, Hortnagel K, Hofmann S, Gekeler F, Scharfe C, Rabl W, Gerbitz KD & Meitinger T. Diabetes insipidus, diabetes mellitus, optic atrophy and deafness (DIDMOAD) caused by mutations in a novel gene (wolframin) coding for a predicted transmembrane protein. *Human Molecular Genetics* 1998 **7** 2021–2028.
5 Takeda K, Inoue H, Tanizawa Y, Matsuzaki Y, Oba J, Watanabe Y, Shinoda K & Oka Y. WFS1 (Wolfram syndrome 1) gene product: predominant subcellular localization to endoplasmic reticulum in cultured cells and neuronal expression in rat brain. *Human Molecular Genetics* 2001 **10** 477–484.
6 Hofmann S, Philbrook C, Gerbitz K-D & Bauer MF. Wolfram syndrome: structural and functional analyses of mutant and wild-type wolframin, the WFS1 gene product. *Human Molecular Genetics* 2003 **12** 2003–2012.
7 Osman AA, Saito M, Makepeace C, Permutt MA, Schlesinger P & Mueckler M. Wolframin expression induces novel ion channel activity in endoplasmic reticulum membranes and increases intracellular calcium. *Journal of Biological Chemistry* 2003 **26** 52755–52762.
8 Chevet E, Cameron PH, Pelletier MF, Thomas DY & Bergeron JJ. The endoplasmic reticulum: integration of protein folding, quality control, signaling and degradation. *Current Opinion in Structural Biology* 2001 **11** 120–124.
9 Rutkowski DT & Kaufman RJ. A trip to the ER: coping with stress. *Trends in Cell Biology* 2004 **14** 20–28.
10 Oyadomari S, Araki E & Mori M. Endoplasmic reticulum stress-mediated apoptosis in pancreatic β-cells. *Apoptosis* 2002 **7** 335–345.
11 Ron D. Proteotoxicity in the endoplasmic reticulum: lessons from the Akita diabetic mouse. *Journal of Clinical Investigation* 2002 **109** 443–445.
12 Yoshioka M, Kayo T, Ikeda T & Koizumi A. A novel locus, Mody 4, distal to D7Mit189 on chromosome 7 determines early-onset NIDDM in nonobese C57BL/6 (Akita) mutant mice. *Diabetes* 1997 **46** 887–894.
13 Wang J, Takeuchi T, Tanaka S, Kubo SK, Kayo T, Lu D, Takata K, Koizumi A & Izumi T. A mutation in the insulin 2 gene induces diabetes with severe pancreatic β-cell dysfunction in the Mody mouse. *Journal of Clinical Investigation* 1999 **103** 27–37.
14 Oyadomari S, Koizumi A, Takeda K, Gotoh T, Akira S, Araki E & Mori M. Targeted disruption of the Chop gene delays endoplasmic reticulum stress–mediated diabetes. *Journal of Clinical Investigation* 2002 **109** 525–532.
15 Ishihara H, Takeda S, Tamura A, Takahashi R, Yamaguchi S, Takei D, Yamada T, Inoue H, Soga H, Katagiri H, Tanizawa Y & Oka Y. Disruption of the WFS1 gene in mice causes progressive β-cell loss and impaired stimulus-secretion coupling in insulin secretion. *Human Molecular Genetics* 2004 **13** 1159–1170.
16 Yamaguchi S, Ishihara H, Tamura A, Yamada T, Takahashi R, Takei D, Katagiri H & Oka Y. Endoplasmic reticulum stress and

N-glycosylation modulate expression of WFS1 protein. *Biochemical and Biophysical Research Communication* 2004 **3** 250–256.
17 Nozaki J, Kubota H, Yoshida H, Naitoh M, Goji J, Yoshinaga T, Mori K, Koizumi A & Nagata K. The endoplasmic reticulum stress response is stimulated through the continuous activation of transcription factors ATF6 and XBP1 in Ins2 + /Akita pancreatic beta cells. *Genes to Cells* 2004 **9** 261–270.
18 Sheng Z, Kawano J, Yanai A, Fujinaga R, Tanaka M, Watanabe Y & Shinoda K. Expression of estrogen receptors (α,β) and androgen receptor in serotonin neurons of the rat and mouse dorsal raphe nuclei; sex and species differences. *Neuroscience Research* 2004 **49** 185–196.
19 Miyazaki J, Araki K, Yamato E, Ikegami H, Asano T, Shibasaki Y, Oka Y & Yamamura K. Establishment of a pancreatic beta cell line that retains glucose-inducible insulin secretion: special reference to expression of glucose transporter isoforms. *Endocrinology* 1990 **127** 126–132.
20 Oka Y, Asano T, Shibasaki Y, Kasuga M, Kanazawa Y & Takaku F. Studies with antipeptide antibody suggest the presence of at least two types of glucose transporter in rat brain and adipocyte. *Journal of Biological Chemistry* 1988 **263** 13432–13439.
21 Li WW, Alexandre S, Cao X & Lee AS. Transactivation of the grp78 promoter by Ca^{2+} depletion. A comparative analysis with A23187 and the endoplasmic reticulum $Ca^{(2+)}$-ATPase inhibitor thapsigargin. *Journal of Biological Chemistry* 1993 **268** 12003–12009.
22 Fujiwara T, Oda K, Yokota S, Takatsuki A & Ikehara Y. Brefeldin A causes disassembly of the Golgi complex and accumulation of secretory proteins in the endoplasmic reticulum. *Journal of Biological Chemistry* 1988 **263** 18545–18552.
23 Zinszner H, Kuroda M, Wang X, Batchvarova N, Lightfoot RT, Remotti H, Stevens JL & Ron D. CHOP is implicated in programmed cell death in response to impaired function of the endoplasmic reticulum. *Genes and Development* 1998 **12** 982–995.
24 McCullough KD, Martindale JL, Klotz LO, Aw TY & Holbrook NJ. Gadd153 sensitizes cells to endoplasmic reticulum stress by downregulating Bcl2 and perturbing the cellular redox state. *Molecular and Cellular Biology* 2001 **21** 1249–1259.
25 Nicholson DW, Ali A, Thornberry NA, Vaillancourt JP, Ding CK, Gallant M, Gareau Y, Griffin PR, Labelle M & Lazebnik YA. Identification and inhibition of the ICE/CED-3 protease necessary for mammalian apoptosis. *Nature* 1995 **376** 37–43.
26 Karasik A, O'Hara C, Srikanta S, Swift M, Soeldner JS, Kahn CR & Herskowitz RD. Genetically programmed selective islet beta-cell loss in diabetic subjects with Wolfram's syndrome. *Diabetes Care* 1989 **12** 135–138.
27 Kinsley BT, Swift M, Dumont RH & Swift RG. Morbidity and mortality in the Wolfram syndrome. *Diabetes Care* 1995 **18** 1566–1570.
28 Gerbitz K-D. Reflexions on a newly discovered diabetogenic gene, wolframin (WFS1). *Diabetologia* 1999 **42** 627–630.
29 Minton JA, Rainbow LA, Ricketts C & Barrett TG. Wolfram syndrome. *Reviews in Endocrine and Metabolic Disorders* 2003 **4** 53–59.
30 Yoshida H, Haze K, Yanagi H, Yura T & Mori K. Identification of the cis-acting endoplasmic reticulum stress response element responsible for transcriptional induction of mammalian glucose-regulated proteins. Involvement of basic leucine zipper transcription factors. *Journal of Biological Chemistry* 1998 **273** 33741–33749.
31 Yoshida H, Okada T, Haze K, Yanagi H, Yura T, Negishi M & Mori K. ATF6 activated by proteolysis binds in the presence of NF-Y (CBF) directly to the cis-acting element responsible for the mammalian unfolded protein response. *Molecular and Cellular Biology* 2000 **20** 6755–6767.
32 Kokame K, Kato H & Miyata T. Identification of ERSE-II, a new cis-acting element responsible for the ATF6-dependent mammalian unfolded protein response. *Journal of Biological Chemistry* 2001 **276** 9199–9205.

Received 24 January 2005
Accepted 7 April 2005

THE JOURNAL OF BIOLOGICAL CHEMISTRY
Vol. 280, No. 18, Issue of May 6, pp. 18525–18535, 2005
Printed in U.S.A.

A Novel Protein Kinase B (PKB)/AKT-binding Protein Enhances PKB Kinase Activity and Regulates DNA Synthesis*

Received for publication, January 18, 2005
Published, JBC Papers in Press, March 7, 2005, DOI 10.1074/jbc.M500586200

Motonobu Anai‡, Nobuhiro Shojima§, Hideki Katagiri¶, Takehide Ogihara¶, Hideyuki Sakoda‡, Yukiko Onishi‡, Hiraku Ono‡, Midori Fujishiro§, Yasushi Fukushima§, Nanao Horike‖, Amelia Viana‖, Masatoshi Kikuchi‡, Noriko Noguchi, Shinichiro Takahashi‡‡, Kuniaki Takata§§, Yoshitomo Oka¶, Yasunobu Uchijima‖, Hiroki Kurihara‖, and Tomoichiro Asano¶¶¶**

*From the ‡Department of Internal Medicine, Institute for Adult Diseases, Asahi Life Foundation, 1-6-1, Marunouchi, Chiyoda-ku, Tokyo 100-0005, Japan, the ¶Division of Molecular Metabolism and Diabetes, Department of Internal Medicine, Tohoku University Graduate School of Medicine, 1-1 Seiryo-cho, Aoba-ku, Sendai, Miyagi 980-8574, Japan, the §§Department of Cell Biology, Institute for Cellular and Molecular Regulation, Gunma University, 3-39-15 Showamachi, Maebashi, Gunma 371-8512, Japan, and the §Department of Internal Medicine, Graduate School of Medicine, **Department of Molecular Biology and Medicine, Research Center for Advanced Science and Technology, ‡‡Department of Animal Sciences, Graduate School of Agriculture and Life Sciences, and ‖Department of Physiological Chemistry and Metabolism, Graduate School of Medicine, University of Tokyo, 7-3-1 Hongo, Bunkyo-ku, Tokyo 113-8655, Japan*

Protein kinase B (PKB)/Akt reportedly plays a role in the survival and/or proliferation of cells. We identified a novel protein, which binds to PKB, using a yeast two-hybrid screening system. This association was demonstrated not only *in vivo* by overexpressing both proteins or by coimmunoprecipitation of the endogenous proteins, but also *in vitro* using glutathione *S*-transferase fusion proteins. Importantly, this protein specifically associates with the C terminus of PKB but not with other AGC kinases and enhances PKB phosphorylation and kinase activation without growth factor stimulation. Thus, we termed this Akt-specific binding protein APE (Akt-phosphorylation enhancer). Since APE-induced phosphorylation of PKB did not occur in cells treated with wortmannin or LY294002, APE itself is not a kinase but seems to enhance or prolong the phosphoinositide 3-kinase-dependent phosphorylation of PKB. In cells in which APE was suppressed by small interfering RNA, DNA synthesis was significantly reduced with suppression of PKB phosphorylation, suggesting a synergistic role of APE in PKB-induced proliferation. On the other hand, in cells overexpressing both PKB and APE, despite markedly increased basal phosphorylation of PKB, both DNA rereplication and subsequent Chk2 phosphorylation and apoptosis were seen, suggesting the involvement of APE in the regulation of cell cycling replication licensing. Taking these observations together, APE appears to be a novel regulator of PKB phosphorylation. Furthermore, the interaction between APE and PKB, possibly dependent on the expression levels of both proteins, may be a novel molecular mechanism leading to proliferation and/or apoptosis.

The serine/threonine protein kinase PKB[1] (also called Akt) is thought to be a key mediator of signal transduction. Upon growth factor stimulation, a family of lipid kinases known as class 1 phosphoinositide 3-kinases (PI 3-kinases) is recruited to the plasma membrane. PI 3-kinases phosphorylate phosphatidylinositol 4,5-bisphosphate at the D-3 position of the inositol ring, converting it to phosphatidylinositol 3,4,5-trisphosphate. Following the activation of PI 3-kinase, PKBs are recruited to the plasma membrane through direct contact of the pleckstrin homology (PH) domain with phosphatidylinositol 3,4,5-trisphosphate and are phosphorylated at Thr^{308} by PDK1 and at Ser^{473} by PDK2, a kinase of which the molecular structure has not yet been identified (1, 2). AGC kinases other than PKB are also known to be regulated by PI 3-kinase, and PKB acts downstream from PI 3-kinase to regulate numerous biological processes, such as proliferation, antiapoptosis, cell growth, and glucose metabolism (1, 2).

PKB has a wide range of substrates, including GSK-3, FKHR (FoxO1), FKHR-L1 (FoxO3), AFX (FoxO4), and eNOS, all of which have the consensus motif RXRXX(S/T) (3, 4). Protein kinases do not generally form stable complexes with their substrates, although PKB has been shown to exist in a stable complex with several of its substrates including MDM2, $p21^{Cip1}$/WAF1, and TSC2 (5–8). It was recently shown that several proteins interact with PKB as function modulators rather than as substrates. In a specific subset of T and B cells, TCL1 interacts with the PH domain of PKB and increases its kinase activity (9). Heat shock protein 90 (Hsp90) was shown to form complexes with Cdc37 and PKB, and PKB was stabilized and protected from dephosphorylation and degradation, resulting in increased kinase activity (10). Carboxyl-terminal modulator protein binds to the carboxyl terminus of PKBα. Carboxyl-terminal modulator protein binding reportedly inhibits the phosphorylation and kinase activity of PKB, and stable expression of carboxyl-terminal modulator protein leads to phenotypic regression of

* This work was supported in part by a grant from Takeda Science Foundation. The costs of publication of this article were defrayed in part by the payment of page charges. This article must therefore be hereby marked "*advertisement*" in accordance with 18 U.S.C. Section 1734 solely to indicate this fact.

¶¶¶ To whom correspondence should be addressed: Dept. of Physiological Chemistry and Metabolism, Graduate School of Medicine, University of Tokyo, 7-3-1 Hongo, Bunkyo-ku, Tokyo 113-8655, Japan. Tel.: 81-3-5841-3603; Fax: 81-3-5803-1874; E-mail: asano-tky@umin.ac.jp.

[1] The abbreviations used are: PKB, protein kinase B; PI, phosphoinositide; PH, pleckstrin homology; GST, glutathione *S*-transferase; PARP, poly(ADP-ribose) polymerase; MTT, 3-[4,5-Dimethylthiazol-2-yl]-2,5-diphenyltetrazolium bromide; GFP, green fluorescent protein; siRNA, small interfering RNA; BrdUrd, bromodeoxyuridine; PKC, protein kinase C.